

# A General Theory of Goodness of Fit in Likelihood Fits

Rajendran Raja

*Fermi National Accelerator Laboratory*

*Batavia, IL 60510*

---

## Abstract

Maximum likelihood fits to data can be performed using binned data and unbinned data. The likelihood fits in either case produce only the fitted quantities but not the goodness of fit. With binned data, one can obtain a measure of the goodness of fit by using the  $\chi^2$  method, after the maximum likelihood fitting is performed. With unbinned data, currently, the fitted parameters are obtained but no measure of goodness of fit is available. This remains, to date, an unsolved problem in statistics. By considering the transformation properties of likelihood functions with respect to change of variable, we conclude that the likelihood ratio of the theoretically predicted probability density to that of *the data density* is invariant under change of variable and provides the goodness of fit. We show how to apply this likelihood ratio for binned as well as unbinned likelihoods and show that even the  $\chi^2$  test is a special case of this general theory. In order to calculate errors in the fitted quantities, we need to solve the problem of inverse probabilities. We use Bayes' theorem to do this, using the data density obtained in the goodness of fit. This permits one to invert the probabilities without the use of a Bayesian prior. The resulting statistics is consistent with frequentist ideas.

---

## Contents

1	Introduction	4
1.1	Notation	4
1.2	To show that $\mathcal{L}$ cannot be used as a goodness of fit variable	5
2	Likelihood ratios	7
2.1	The concept of “data likelihood” derived from the <i>pdf</i> of the data	7
2.2	Historical use of Likelihood Ratios	10
3	Normalizing the theoretical curve to the data	10
4	Binned Goodness of Fit	11
4.1	The multinomial distribution	11
4.2	Degeneracy of the distribution	11
4.3	To Show that the Binned Negative Log-Likelihood Ratio Approaches a $\chi^2$ Distribution for Large $n$	
4.4	Normalizing theory and experiment and the problem of Goodness of fit for the Poisson distribution	
4.5	The Gaussian limit of the binomial	17
4.6	To show that $\chi^2$ is also the negative logarithm of a likelihood ratio	18
5	Unbinned Goodness of Fit	19
5.1	An illustrative example	21
5.2	Iterative Determination of the Smoothing Factor	23

---

*Email address:* `raja@fnal.gov` (Rajendran Raja).

5.3	An Empirical Measure of the Goodness of Fit	25
5.4	Improving the $PDE$	27
5.5	Periodic Boundary Conditions	29
6	The distribution of the goodness of fit variable	32
7	Calculation of fitted errors	33
7.1	Derivation of Bayes' theorem equations	33
7.2	The Bayesian Paradigm	37
7.3	The New Paradigm	40
7.4	The two different methods to obtain $\mathcal{P}_n(s^*)$	52
7.5	Co-ordinate transformations $s^{*'} = s^{*'}(s^*)$	54
8	Conclusions	55
9	Acknowledgments	57
10	Appendix	57
10.1	An extreme problem	57
10.2	Goodness of fit for the above problem	57
10.3	Comments	59
	References	59

## 1 Introduction

In particle physics as well as other branches of science, fitting theoretical models to data is a crucial end stage to the performance of experiments. Minimizing the  $\chi^2$  between theory and experiment is perhaps the most commonly used form of fitting, with data binned in histograms. Such fits yield not only the fitted parameters and errors on the fitted parameters but also a measure of the goodness of fit. Another common fitting method is the maximum likelihood method which can be performed on binned and unbinned data to obtain the best values of theoretical parameters. In the case of unbinned likelihood fitting, there is currently no measure of the goodness of fit. In this paper, we propose a solution to the problem, which by its nature works generally for both binned and unbinned likelihood fits. A general theory of goodness of fit in likelihood fits results.

### 1.1 Notation

In what follows, we will denote by the vector  $s$ , the theoretical parameters ( $s$  for “signal”) and the vector  $c$ , the experimentally measured quantities or “configurations”. For simplicity, we will illustrate the method where both  $s$  and  $c$  are one dimensional, though either or both can be multi-dimensional in practice. We thus define the theoretical model by the conditional probability density  $P(c|s)$ , defined as the probability of observing  $c$  given a value of  $s$ . The theoretical probability function obeys the normalization condition

$$\int P(c|s)dc = 1 \tag{1}$$

Then an unbinned maximum likelihood fit to data is obtained by maximizing the likelihood [1],

$$\mathcal{L} = \prod_{i=1}^{i=n} P(c_i|s) \quad (2)$$

where the likelihood is evaluated at the  $n$  observed data points  $c_i, i = 1, n$ . Such a fit will determine the maximum likelihood value  $s^*$  of the theoretical parameters, but will not tell us how good the fit is.

### 1.2 To show that $\mathcal{L}$ cannot be used as a goodness of fit variable

The goodness of fit variable must be invariant under a change of variable  $c \rightarrow c'$ . The value of the likelihood  $\mathcal{L}$  at the maximum likelihood point does not furnish a goodness of fit, since the likelihood is not invariant under change of variable. This can be seen by observing that one can transform the variable set  $c$  to a variable set  $c'$  such that  $P(c'|s^*)$  is uniformly distributed between 0 and 1. In one dimension, this is trivially done by the transformation function  $c'(c)$  such that

$$c'(c) = \int_{c_1}^c P(t|s^*) dt \quad (3)$$

The variable  $c$  ranges from  $c_1$  to  $c_2$  and the probability function  $P(c|s^*)$  normalizes to unity in this range. This implies that  $c'$  ranges from 0 to 1. Such a transformation is known as a hypercube transformation, in multi-dimensions. The transformed probability distribution in the variable  $c'$  is unity in this interval as can be seen by examining the Jacobian of the transformation  $|\frac{\partial c'}{\partial c}|$

$$|\frac{\partial c'}{\partial c}| = P(c|s^*) \quad (4)$$

$$P(c'|s^*) = P(c|s^*) \left| \frac{\partial c}{\partial c'} \right| = 1 \quad (5)$$

Other datasets will yield different values of likelihood in the variable space  $c$  when the likelihood is computed with the original function  $P(c|s^*)$ . However, in hypercube space, the value of the likelihood is unity regardless of the dataset  $c'_i, i = 1, n$ , thus the likelihood  $\mathcal{L}$  cannot furnish a goodness of fit by itself, since neither the likelihood, nor ratios of likelihoods computed using the same distribution  $P(c|s^*)$  is invariant under variable transformations. The fundamental reason for this non-invariance is that only a single distribution, namely,  $P(c|s^*)$  is being used to compute the goodness of fit.

To illustrate further, we use a concrete example of fitting a dataset using the maximum likelihood method as shown in Figure 1(a). The fitting is done in the range  $c_1 < c < c_2$ , where  $c_1 = 1.0$  and  $c_2 = 5.0$ . The fitting function is

$$P(c|s) = \frac{\exp(-c/s)}{s(\exp(-c_1/s) - \exp(-c_2/s))} \quad (6)$$

which normalizes to unity in the range  $c_1 < c < c_2$ . The fitted dataset is shown as a full histogram. The dashed histogram shows a dataset that is a poor fit to the data and will produce a smaller value of  $\mathcal{L}$  when fitted as a function of  $c$ . Figure 1(b) shows the same data in the hypercube space where the fitted function is flat as per the transformation given in equation 3. Both the datasets will produce a value of unity for  $\mathcal{L}$  in this space implying an equally good fit in either case, which is obviously false. This clearly demonstrates that the likelihood by itself cannot provide a goodness of fit variable.

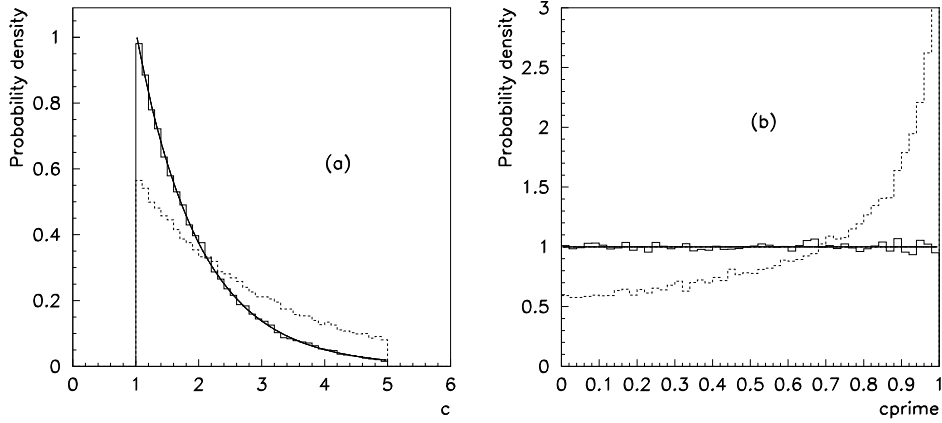


Fig. 1. (a) shows the fitting in the dataset space. The curve shows the fitted function. Superimposed is the fitted data, (full histogram, normalized to unity). The dashed histogram shows the different dataset which obviously does not fit to the fitted curve. (b) The same plot in hyperspace. The fitted function is flat by construction. Both the fitted data set (full histogram) and the dashed histogram will have the same value of likelihood  $\mathcal{L}$  in this space which implies that  $\mathcal{L}$  cannot be used as a goodness of fit variable.

## 2 Likelihood ratios

### 2.1 The concept of “data likelihood” derived from the pdf of the data

It is interesting to note that while using  $\chi^2$  as the goodness of fit technique for binned histograms, we use two distribution functions, namely the theoretical curve and the data. By binning the data, we are in effect estimating the probability density function of the data as the second distribution, in addition to the theoretical distribution specified by the theoretical curve. In likelihood language we define the probability density function (*pdf*) of the data as

$$P^{data}(c) = \lim_{N \rightarrow \infty} \frac{1}{N} \frac{dN}{dc} \quad (7)$$

where  $N$  is the number of times the experiment is repeated that results in the observable  $c$ . The function  $P^{data}(c)$  obeys the normalization condition

$$\int P^{data}(c)dc = 1 \quad (8)$$

When one is using binned likelihoods, the *pdf* of the data would be estimated by binning the events in a histogram and normalizing the sum of contents of all bins to unity. In the unbinned case, we will describe below a technique [2] on estimating  $P^{data}(c)$  using Probability Density Estimators (*PDE*).

We can now define a likelihood ratio  $\mathcal{L}_{\mathcal{R}}$  such that

$$\mathcal{L}_{\mathcal{R}} = \frac{\prod_{i=1}^{i=n} P(c_i|s)}{\prod_{i=1}^{i=n} P^{data}(c_i)} \equiv \frac{P(\vec{c}_n|s)}{P^{data}(\vec{c}_n)} \quad (9)$$

where we have used the notation  $\vec{c}_n$  to denote the dataset  $c_i, i = 1, n$ .

Since the  $n$  events  $c_i, i = 1, n$  are independent, the probability of obtaining the dataset  $\vec{c}_n$  is given by

$$P^{data}(\vec{c}_n) = \prod_{i=1}^{i=n} P^{data}(c_i) \quad (10)$$

The quantity  $P^{data}(\vec{c}_n)$  we name the “data likelihood” of the dataset  $\vec{c}_n$  and the quantity  $P(\vec{c}_n|s)$  as the “theory likelihood” of the dataset  $\vec{c}_n$ . We note that the “data likelihood”  $P^{data}(\vec{c}_n)$  may also be thought of as the probability density of the “ $n$  – object”  $\vec{c}_n$  which obeys the normalization condition

$$\int P^{data}(\vec{c}_n) d\vec{c}_n = 1 \quad (11)$$

Let us now note that  $\mathcal{L}_{\mathcal{R}}$  is invariant under a general variable transformation (not restricted to hypercube transformation)  $c \rightarrow c'$ , since



$$P(c'|s) = \left| \frac{\partial c}{\partial c'} \right| P(c|s) \quad (12)$$

$$P^{data}(c') = \left| \frac{\partial c}{\partial c'} \right| P^{data}(c) \quad (13)$$

$$\mathcal{L}'_{\mathcal{R}} = \mathcal{L}_{\mathcal{R}} \quad (14)$$

and the Jacobian of the transformation  $\left| \frac{\partial c}{\partial c'} \right|$  cancels in the numerator and denominator in the ratio. This is an extremely important property of the likelihood ratio  $\mathcal{L}_{\mathcal{R}}$  that qualifies it to be a goodness of fit variable. Later, we will show that the binned likelihood ratio asymptotically approaches a  $\chi^2$  distribution as the number of events  $n \rightarrow \infty$ , further motivating this choice. Since the denominator  $P^{data}(\vec{c}_n)$  is independent of the theoretical parameters  $s$ , both the likelihood ratio and the likelihood maximize at the same point  $s^*$ . The likelihood ratios for two different data sets  $\vec{c}_m$  and  $\vec{c}_n$  can be combined by multiplication as per

$$\mathcal{L}_{\mathcal{R}}^{m+n} = \mathcal{L}_{\mathcal{R}}^m \times \mathcal{L}_{\mathcal{R}}^n \quad (15)$$

This rule follows from the definition of  $\mathcal{L}_{\mathcal{R}}$  in equation 9. In practice, we will use the negative log-likelihood ratio  $\mathcal{NLLR} = -\log_e \mathcal{L}_{\mathcal{R}}$  as the goodness of fit variable and minimize it. The multiplication rule of equation 15 results in an addition rule for  $\mathcal{NLLR}$ . The problem of finding the distribution of  $\mathcal{NLLR}$  for a good fit then reduces to finding the distribution of  $\mathcal{NLLR}$  in hyper-cube space for a variable that is uniformly distributed between zero and one, as in Figure 1(b). This is because  $\mathcal{NLLR}$  is invariant under the transformation of variable. So all goodness of fit problems using likelihood ratios can be reduced to finding the distribution of  $\mathcal{NLLR}$  for a variable that is uniformly distributed in hypercube space.

## 2.2 *Historical use of Likelihood Ratios*

The Neyman-Pearson lemma [3] states that if one is trying to choose between two hypotheses  $H_0$  and  $H_1$ , then the cut on the likelihood ratio

$$\mathcal{L}_R = \frac{P(\vec{c}_n|H_0)}{P(\vec{c}_n|H_1)} > \epsilon \quad (16)$$

will have the optimum power in differentiating between the hypotheses  $H_0$  and  $H_1$ , where  $\epsilon$  is a constant adjusted to obtain the desired purity in favor of hypothesis  $H_0$ . Notice that this likelihood ratio is between the likelihood computed for two different hypotheses  $H_0$  and  $H_1$ . Our likelihood ratio differs fundamentally from this in that the denominator we use  $P(\vec{c}_n)$  is the “data likelihood” that is computed from the distribution of the data and is not tied to any hypothesis as such.

## 3 **Normalizing the theoretical curve to the data**

The method of maximum likelihood fits the shape of the theoretical distribution to the data distribution. The theoretical model obeys the normalization condition in equation 1 and the likelihood is evaluated at the number of observed data events  $n$ . There is no explicit mention of the theoretically expected number of events, which we denote by  $n_t$ . Later we will show how to incorporate a goodness of fit in the absolute normalization by making use of the binomial distribution and its limiting cases the Poisson and the normal distributions. We will begin by obtaining goodness of fit formulae for the case where we bin the data and fit the theoretical shape to the experimental distribution.

## 4 Binned Goodness of Fit

When one bins data in histograms and fits the theory shape to the data, one can fit by using either maximum likelihood or by minimizing  $\chi^2$ . In either case, the goodness of fit is usually evaluated using  $\chi^2$ . We now illustrate how the likelihood ratio defined in section 2 can be used to obtain a goodness of fit after the maximum likelihood fitting is done. In order to evaluate the likelihood ratio, one needs to evaluate the theory likelihood and the data likelihood for each value of  $c_i$ . For the binned histogram, we make the approximation of assuming that both these quantities are constant for all values of  $c_i$  in a given bin and evaluating each at the bin center. Let there be  $n_b$  bins and let the  $k^{th}$  bin contain  $n_k$  entries.

### 4.1 The multinomial distribution

The probability of obtaining the histogram is given by the multinomial distribution

$$P(histogram) = \frac{n!}{\prod_{k=1}^{k=n_b} n_k!} \prod_{k=1}^{k=n_b} P(c_k|s)^{n_k} \quad (17)$$

$$\sum_{k=1}^{k=n_b} n_k = n \quad (18)$$

### 4.2 Degeneracy of the distribution

The factor  $\frac{n!}{\prod_{k=1}^{k=n_b} n_k!}$  denotes the number of ways  $n$  events can be partitioned to form the observed histogram, which we term the degeneracy  $\mathcal{D}$  of the histogram. Each of the  $\mathcal{D}$  histograms is identical to each other and possesses the

same goodness of fit. We can then evaluate the goodness of fit for any one of the  $\mathcal{D}$  degenerate histograms, the likelihood for which is given by

$$\mathcal{L} = \prod_{k=1}^{k=n_b} P(c_k|s)^{n_k} \quad (19)$$

and the likelihood ratio can be written as

$$\mathcal{L}_R = \prod_{k=1}^{k=n_b} \left( \frac{P(c_k|s)}{P^{data}(c_k)} \right)^{n_k} \quad (20)$$

The value of  $\frac{P(c_k|s)}{P^{data}(c_k)}$  raised to the power  $n_k$  in equation 20 results from the fact that there are  $n_k$  configurations  $c_i$  in the  $k^{th}$  bin and we are multiplying a constant ratio (at the bin center) over  $n_k$  configurations. If  $\Delta c_k$  is the bin width for the  $k^{th}$  bin, then the data likelihood can be approximated by

$$P^{data}(c_k) \approx \frac{n_k}{n\Delta c_k} \quad (21)$$

This obeys the normalization condition

$$\int P^{data}(c_k)dc_k \approx \sum_{k=1}^{k=n_b} \frac{n_k}{n\Delta c_k} \Delta c_k = 1. \quad (22)$$

The theoretical likelihood can be integrated over the bin to yield

$$P^{bin\ average}(c_k|s) = \frac{1}{\Delta c_k} \int_{c=c_k-\Delta c_k/2}^{c=c_k+\Delta c_k/2} P(c|s)dc \quad (23)$$

This obeys the normalization condition

$$\sum_{k=1}^{k=n_b} P^{bin\ average}(c_k|s)\Delta c_k = 1 \quad (24)$$

Then the likelihood ratio can be written

$$\mathcal{L}_R = \prod_{k=1}^{k=n_b} \left( \frac{n\Delta c_k P^{bin\ average}(c_k|s)}{n_k} \right)^{n_k} \equiv \prod_{k=1}^{k=n_b} \left( \frac{T_k}{n_k} \right)^{n_k} \quad (25)$$

where  $T_k \equiv n \Delta c_k P^{bin\ average}(c_k|s)$  is the theoretically expected number of events in the  $k^{th}$  bin obeying the normalization condition  $\sum_k T_k = n$ , as per equation 24. This likelihood ratio may be used to obtain a maximum likelihood fit as well as to obtain a goodness of fit. Note that the likelihood ratio is well-behaved even for empty bins where  $n_k = 0$ , since  $n_k^{n_k}$  is unity for such cases.

Note that the negative log-likelihood ratio  $\mathcal{NLLR}$  resulting from equation 25 yields

$$\mathcal{NLLR} = \sum_{k=1}^{k=n_b} n_k \log_e \left( \frac{n_k}{T_k} \right) \quad (26)$$

which is the same result as derived by Baker and Cousins [4] for the multinomial case where normalization is preserved between theory and experiment. We have derived the result using very different arguments (than Baker and Cousins) for the denominator of the likelihood ratio, namely it is the value of the *data pdf* at the bin center as a result of the general theory developed here.

If we are reluctant to work out (for reasons of computing speed) the integral in equation 23 for each bin at each step of the fitting process, then we can approximate it by the bin center values

$$P^{bin\ average}(c_k|s) \approx \frac{P(c_k|s)}{\sum_k P(c_k|s) \Delta c_k} \quad (27)$$

This then obeys the normalization equation 24 and the expression in equation 26 for  $\mathcal{NLLR}$  can be used generally.

4.3 To Show that the Binned Negative Log-Likelihood Ratio Approaches a  $\chi^2$  Distribution for Large  $n$

Let the difference between  $n_k$ , the observed number of events and  $T_k$  the theoretical number of events be denoted by  $\lambda_k = n_k - T_k$ . Then  $\sum_k \lambda_k = 0$ , by virtue of the normalization conditions. Then the binned negative log likelihood ratio  $\mathcal{NLLR}$  can be written

$$\mathcal{NLLR} = -\log_e \mathcal{L}_R = - \sum_{k=1}^{k=n_b} n_k \log_e \left( 1 - \frac{\lambda_k}{n_k} \right) \quad (28)$$

This can be expanded in powers of  $\lambda_k/n_k$  as

$$\mathcal{NLLR} = -\log_e \mathcal{L}_R = \sum_{k=1}^{k=n_b} n_k \left( \frac{\lambda_k}{n_k} + \frac{1}{2} \left( \frac{\lambda_k}{n_k} \right)^2 + \frac{1}{3} \left( \frac{\lambda_k}{n_k} \right)^3 + \frac{1}{4} \left( \frac{\lambda_k}{n_k} \right)^4 \dots \right) \quad (29)$$

$$= \sum_{k=1}^{k=n_b} \frac{1}{2} \left( \frac{\lambda_k^2}{n_k} \right) + \frac{1}{3} \left( \frac{\lambda_k^3}{n_k^2} \right) + \frac{1}{4} \left( \frac{\lambda_k^4}{n_k^3} \right) \dots \quad (30)$$

As  $n \rightarrow \infty$ , the individual bin contents become normally distributed about their expected value  $T_k$  with variance  $\sigma_k^2 = n_k(1 - n_k/n) \approx n_k$  for  $n_k \ll n$ . This is true for all cases (named the *null hypothesis*) where the data and theory fit each other. Then we can write  $\chi_k^2 = \lambda_k^2/n_k$  and

$$\mathcal{NLLR} = \sum_{k=1}^{k=n_b} \frac{1}{2} \chi_k^2 + \frac{1}{3} \frac{\lambda_k^3}{\sigma_k^4} + \frac{1}{4} \frac{\lambda_k^4}{\sigma_k^6} \dots \quad (31)$$

For large  $n$ ,  $\lambda_k \approx \sqrt{n_k}$  and the higher order terms may be neglected yielding

$$\mathcal{NLLR} \rightarrow \sum_{k=1}^{k=n_b} \frac{1}{2} \chi_k^2 \text{ when } n \rightarrow \infty \quad (32)$$

This is an example of the likelihood ratio theorem [5]. The expected value of the  $\mathcal{NLLR}$  can then be written

$$E(\mathcal{NLLR}) = \sum_{k=1}^{k=n_b} \frac{1}{2} E(\chi_k^2) + \frac{1}{3} \frac{\mu_3}{\sigma_k^4} + \frac{1}{4} \frac{\mu_4}{\sigma_k^6} + \frac{1}{5} \frac{\mu_5}{\sigma_k^8} + \frac{1}{6} \frac{\mu_6}{\sigma_k^{10}} \dots \quad (33)$$

where  $\mu_3, \mu_4, \dots$  are the  $3^{rd}, 4^{th} \dots$  moments of the normal distribution about the mean. Since the normal distribution is symmetric about the mean, all the odd moments ( $\mu_3, \mu_5 \dots$ ) are zero. The even moments of the normal distribution (for integer  $l$ ) are given by the formula

$$\mu_{2l} = 1.3.5 \dots (2l-1) \sigma^{2l} \quad (34)$$

This yields

$$E(\mathcal{NLLR}) = \sum_{k=1}^{k=n_b} \frac{1}{2} E(\chi_k^2) + \frac{3}{4} \frac{\sigma_k^4}{\sigma_k^6} + \frac{15}{6} \frac{\sigma_k^8}{\sigma_k^{10}} \dots \quad (35)$$

All the remaining terms tend to zero as  $1/n_k (= 1/\sigma_k^2)$  as  $n_k \rightarrow \infty$  leading to

$$E(\mathcal{NLLR}) = \sum_{k=1}^{k=n_b} \frac{1}{2} E(\chi_k^2) = \frac{n_b}{2} \quad (36)$$

$$E(\mathcal{L}_R) = \exp(-n_b/2) \quad (37)$$

The number of degrees of freedom for  $\mathcal{NLLR}$  would be  $n_b - 1$ , due to the normalization condition  $\sum_k n_k = n$ .

#### 4.4 *Normalizing theory and experiment and the problem of Goodness of fit for the Poisson distribution*

As we have pointed out, maximum likelihood fitting only fits the shape of the theoretical distribution to the experimental data. This is due to the normal-

ization condition of equation 1. However, if we employ a binomial distribution and define the first bin as containing the number of observed events  $n$  with theoretical expectation of  $n_t$  events, and the second bin to contain the number of unobserved events in  $N$  tries, then one can employ the formula in equation 25 with  $n_b = 2$  to obtain the likelihood ratio.

$$\mathcal{L}_R = \left(\frac{n_t}{n}\right)^n \left(\frac{N - n_t}{N - n}\right)^{N-n} = \left(\frac{n_t}{n}\right)^n \left(\frac{1 - n_t/N}{1 - n/N}\right)^{N-n} \quad (38)$$

We now take the Poissonian limit of  $N \rightarrow \infty$  with  $n_t$  and  $n$  finite and the above likelihood ratio becomes

$$\mathcal{L}_R = e^{-(n_t-n)} \left(\frac{n_t}{n}\right)^n \quad (39)$$

where we have employed the relations  $(N - n) \rightarrow N$  and  $(1 - x/N)^N \rightarrow e^{-x}$  as  $N \rightarrow \infty$ .

Equation 39 provides the goodness of fit likelihood ratio for all Poissonian problems where  $n_t$  events are expected and  $n$  are observed. We can now multiply this Poissonian  $\mathcal{L}_R$  with equation 25 to produce the likelihood ratio for a general binned likelihood problem where the normalization for theory and experiment vary.

$$\mathcal{L}_R = e^{-(n_t-n)} \left(\frac{n_t}{n}\right)^n \prod_{k=1}^{k=n_b} \left(\frac{T_k}{n_k}\right)^{n_k} = e^{-(n_t-n)} \prod_{k=1}^{k=n_b} \left(\frac{T'_k}{n_k}\right)^{n_k} \quad (40)$$

where we have defined  $T'_k = n_t T_k / n$  and  $\sum T'_k = n_t$ . With this redefinition, we obtain the  $\mathcal{NLLR}$  for the multinomial with theoretical normalization differing from the experimental one as

$$\mathcal{NLLR} = \sum_{k=1}^{k=n_b} T'_k - n_k + n_k \log_e \left(\frac{n_k}{T'_k}\right) \quad (41)$$



This is same as the “Poissonian result” of Baker and Cousins [4] again derived using very different arguments for the denominator of the likelihood ratio.

#### 4.5 The Gaussian limit of the binomial

The Poissonian result is useful when  $n_t$  and  $n$  are relatively small numbers ( $< \approx 25$ ). When we have larger number of events, then the Gaussian approximation is more relevant. We have already shown that (equation 30) that in a multinomial, the negative log likelihood ratio can be approximated by

$$\mathcal{NLLR} = \sum_{k=1}^{k=n_b} \frac{1}{2} \left( \frac{\lambda_k^2}{n_k} \right) \quad (42)$$

We apply this to the binomial with  $n_b = 2$ ,  $n_1 = n$ , and  $n_2 = N - n$  and  $\lambda_1 = -\lambda_2 = n - n_t$ . Then

$$\mathcal{NLLR} = \frac{\lambda_2^2}{2} \left( \frac{1}{n_1} + \frac{1}{n_2} \right) = \frac{\lambda_2^2}{2} \left( \frac{1}{(1 - n/N)(n/N)N} \right) \quad (43)$$

$$\approx \frac{\lambda_2^2}{2} \left( \frac{1}{Npq} \right) = \frac{(n - n_t)^2}{2\sigma^2} \quad (44)$$

where  $p = n_t/N \approx n/N$  is the probability of an event appearing in the first bin and  $q = 1 - p$  and  $\sigma^2 = Npq$  is the variance of the bin contents of the first bin. We now let  $N \rightarrow \infty$ ,  $n \rightarrow \infty$  and  $N \gg n$ . In this case, the variance can be approximated by  $n$  and we have the Gaussian case with  $\mathcal{NLLR} = (n - n_t)^2/2n$ . This  $\mathcal{NLLR}$  can be added to the one resulting from the maximum likelihood shape fitting to get an overall goodness of fit.

We must emphasize once again that the method of maximum likelihood always fits theoretical shapes to experimental data. We have been able to circumvent this restriction by using the device of the binomial distribution where the

observed events  $n$  are in the first bin and the total number of events in the distribution  $N$  refer to the “number of tries” and the second bin consists of the  $N - n$  events that failed to appear in the experiment. The binomial distribution is special in this regard since once we specify the properties of the first bin, the second bin is completely specified and anti-correlated with the first bin. The number of tries is unknown, but we set it to infinity in two different limits as discussed resulting in the Poisson and the Gaussian likelihood ratios.

#### 4.6 To show that $\chi^2$ is also the negative logarithm of a likelihood ratio

The most commonly used method for goodness of fit is the  $\chi^2$  test of Karl Pearson, which is used even when the quantities being fitted are not events but measurements with error bars. We show here that the  $\chi^2$  measure is also twice the negative logarithm of a Gaussian likelihood *ratio* rather than the negative logarithm of a Gaussian likelihood, as is the popular misconception. Consider a binned histogram where the contents in the  $k^{th}$  bin is noted by  $c_k$  and the theoretical expectation of this bin is  $s_k$ . The standard error of the observed variable  $c_k$  is known to be  $\sigma_k$ . Then, one can write

$$P(c_k|s_k) = \frac{1}{\sqrt{2\pi}\sigma_k} \exp\left(-\frac{(c_k - s_k)^2}{2\sigma_k^2}\right) = \frac{1}{\sqrt{2\pi}\sigma_k} \exp\left(-\frac{\chi_k^2}{2}\right) \quad (45)$$

This leads to

$$-\log_e(P(c_k|s_k)) = \frac{\chi_k^2}{2} + \log_e(\sqrt{2\pi}\sigma_k) \quad (46)$$

From the above expression, people are mistakenly led to conclude that  $\chi^2$  is equivalent to twice the negative log-likelihood. This ignores the term  $\log_e(\sqrt{2\pi}\sigma_k)$  in the above equation, which varies from bin to bin. In order to work out the

likelihood ratio, we need to estimate the data density  $P(c_k)$  at each measurement. The data points are distributed as a Gaussian with standard deviation  $\sigma_k$ . The best estimate of the mean of the Gaussian from the data alone is  $c_k$ . This leads to

$$P(c_k) = \frac{1}{\sqrt{2\pi}\sigma_k} \exp\left(-\frac{(c_k - c_k)^2}{2\sigma_k^2}\right) = \frac{1}{\sqrt{2\pi}\sigma_k} \quad (47)$$

yielding the likelihood ratio

$$\mathcal{L}_R^k = \frac{P(c_k|s_k)}{P(c_k)} = \exp\left(-\frac{(s_k - c_k)^2}{2\sigma_k^2}\right) = \exp\left(-\frac{\chi_k^2}{2}\right) \quad (48)$$

The overall likelihood ratio is given by

$$\mathcal{L}_R = \prod_{k=1}^{k=n_b} \mathcal{L}_R^k \quad (49)$$

leading to

$$\chi^2 = 2 \log_e(\mathcal{L}_R) = \sum_{k=1}^{k=n_b} \chi_k^2 \quad (50)$$

i.e.  $\chi^2$  is equal to twice the negative log-likelihood ratio and not the negative log-likelihood!.

## 5 Unbinned Goodness of Fit

Very often the data are not plentiful enough to bin adequately and it is more efficient to perform an unbinned likelihood fit. Presently, a goodness of fit method does not exist for unbinned likelihood fits. Using the formalism developed above, we present a solution. After the unbinned likelihood fit is performed by maximizing the likelihood in equation 2 one needs to work out

the *data likelihood*  $P^{data}(\vec{c}_n)$  in order to evaluate the likelihood ratio and the goodness of fit. We employ the technique of Probability Density Estimators (*PDE's*), also known as Kernel Density Estimators [2] (*KDE's*) to do this. The *pdf*  $P^{data}(c)$  is approximated by

$$P^{data}(c) \approx PDE(c) = \frac{1}{n} \sum_{i=1}^{i=n} \mathcal{G}(c - c_i) \quad (51)$$

where a Kernel function  $\mathcal{G}(c - c_i)$  is centered around each data point  $c_i$ , is so defined that it normalizes to unity. The choice of the Kernel function can vary depending on the problem. A popular kernel is the Gaussian defined in the multi-dimensional case as

$$\mathcal{G}(c) = \frac{1}{(\sqrt{2\pi}h)^d \sqrt{\det(E)}} \exp\left(\frac{-H^{\alpha\beta} c^\alpha c^\beta}{2h^2}\right) \quad (52)$$

where  $E$  is the error matrix of the data defined as

$$E^{\alpha,\beta} = \langle c^\alpha c^\beta \rangle - \langle c^\alpha \rangle \langle c^\beta \rangle \quad (53)$$

and the  $\langle \rangle$  implies average over the  $n$  events, and  $d$  is the number of dimensions. The Hessian matrix  $H$  is defined as the inverse of  $E$  and the repeated indices imply summing over. The parameter  $h$  is a “smoothing parameter”, which has[6] a suggested optimal value  $h \propto n^{-1/(d+4)}$ , that satisfies the asymptotic condition

$$\mathcal{G}_\infty(c - c_i) \equiv \lim_{n \rightarrow \infty} \mathcal{G}(c - c_i) = \delta(c - c_i) \quad (54)$$

The parameter  $h$  will depend on the local number density and will have to be adjusted as a function of the local density to obtain good representation of the data by the *PDE*. Our proposal for the goodness of fit in unbinned likelihood

fits is thus the likelihood ratio

$$\mathcal{L}_{\mathcal{R}} = \frac{P(\vec{c}_n|s)}{P^{data}(\vec{c}_n)} \approx \frac{P(\vec{c}_n|s)}{P^{PDE}(\vec{c}_n)} \quad (55)$$

evaluated at the maximum likelihood point  $s^*$ .

### 5.1 An illustrative example

We consider a simple one-dimensional case where the data is an exponential distribution, say decay times of a radioactive isotope. The theoretical prediction is given by

$$P(c|s) = \frac{1}{s} \exp\left(-\frac{c}{s}\right) \quad (56)$$

We have chosen an exponential with  $s = 1.0$  for this example. The Gaussian Kernel for the  $PDE$  would be given by

$$\mathcal{G}(c) = \frac{1}{(\sqrt{2\pi}\sigma h)} \exp\left(-\frac{c^2}{2\sigma^2 h^2}\right) \quad (57)$$

where the variance  $\sigma$  of the exponential is numerically equal to  $s$ . To begin with, we chose a constant value for the smoothing parameter, which for 1000 events generated is calculated to be 0.125. Figure 2 shows the generated events, the theoretical curve  $P(c|s)$  and the  $PDE$  curve  $P(c)$  normalized to the number of events. The  $PDE$  fails to reproduce the data near the origin due to the boundary effect, whereby the Gaussian probabilities for events close to the origin spill over to negative values of  $c$ . This lost probability would be compensated by events on the exponential distribution with negative  $c$  if they existed. In our case, this presents a drawback for the  $PDE$  method, which we

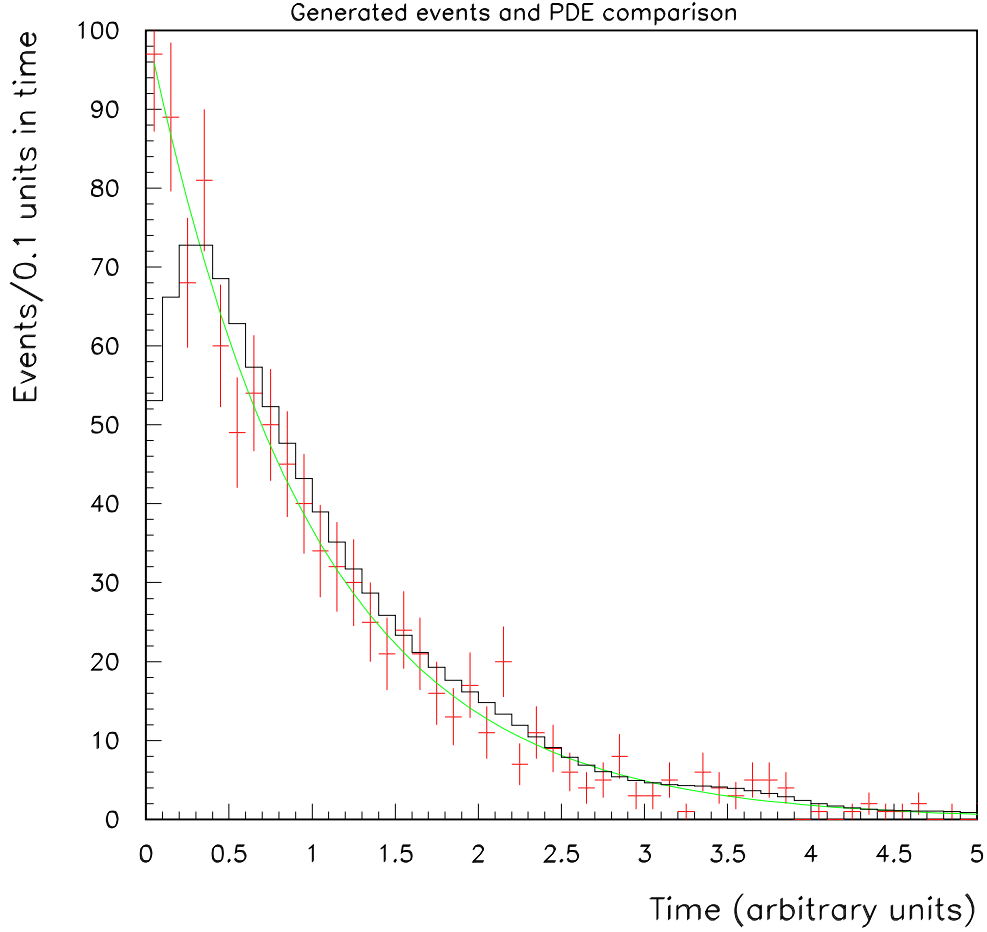


Fig. 2. Figure shows the histogram (with errors) of generated events. Superimposed is the theoretical curve  $P(c|s)$  and the  $PDE$  estimator (solid) histogram with no errors.

will remedy later in the paper using  $PDE$  definitions on the hypercube and periodic boundary conditions. For the time being, we will confine our example to values of  $c > 1.0$  to avoid the boundary effect.

In order to test the goodness of fit capabilities of the likelihood ratio  $\mathcal{L}_{\mathcal{R}}$ , we superimpose a Gaussian on the exponential and try and fit the data by a simple exponential. Figure 5 shows the “data” with 1000 events generated as

an exponential in the fiducial range  $1.0 < c < 5.0$ . Superimposed on it is a Gaussian of 500 events. More events in the exponential are generated in the interval  $0.0 < c < 1.0$  to avoid the boundary effect at the fiducial boundary at  $c=1.0$ . Since the number density varies significantly, we have had to introduce a method of iteratively determining the smoothing factor as a function of  $c$ .

## 5.2 Iterative Determination of the Smoothing Factor

The expression  $h \approx n^{-1/(d+4)}$  clearly is meant to give a smoothing factor that decreases slowly with increased statistics  $n$ . It is expected to be true on average over the whole distribution. However, the exponential distribution under consideration has event densities that vary by orders of magnitude as a function of the time variable  $c$ . In order to obtain a function  $h(c)$  that takes into account this variation, we first work out a *PDE* with constant  $h$  and then use the number densities obtained thus [8] to obtain  $h(c)$  as per the equation

$$h(c) = \left( \frac{n \text{PDE}(c)}{(c_2 - c_1)} \right)^{-0.6} \quad (58)$$

The equation is motivated by the consideration that a uniform distribution of events between  $c_1$  and  $c_2$  has a *pdf*  $= 1/(c_2 - c_1)$  whereas the real *pdf* is approximated by *PDE*. The function  $h(c)$  thus obtained is used to work out a better *PDE*( $c$ ). This process is iterated three times to give the best smoothing function.

We generate  $n=1000$  events in the fiducial interval. If now we were to superimpose a Gaussian with 500 events centered at  $c=2.0$  and width=0.2 on the data, the *PDE* estimator will follow the data as shown in Figure 5. This shows that the *PDE* estimator we have is adequate to reproduce the data, once the

smoothing parameter is made to vary with the number density appropriately. The smoothing function  $h(c)$  for the events in Figure 5 is shown in Figure 3. It can be seen that the value of  $h$  increases for regions of low statistics and decreases for regions of high statistics. Superimposed is the constant smoothing factor obtained by the equation  $h \approx 0.5n^{-1/(d+4)} = 0.5n^{-0.2}$ , with  $n$  being the total number of events generated, including those outside the fiducial volume.

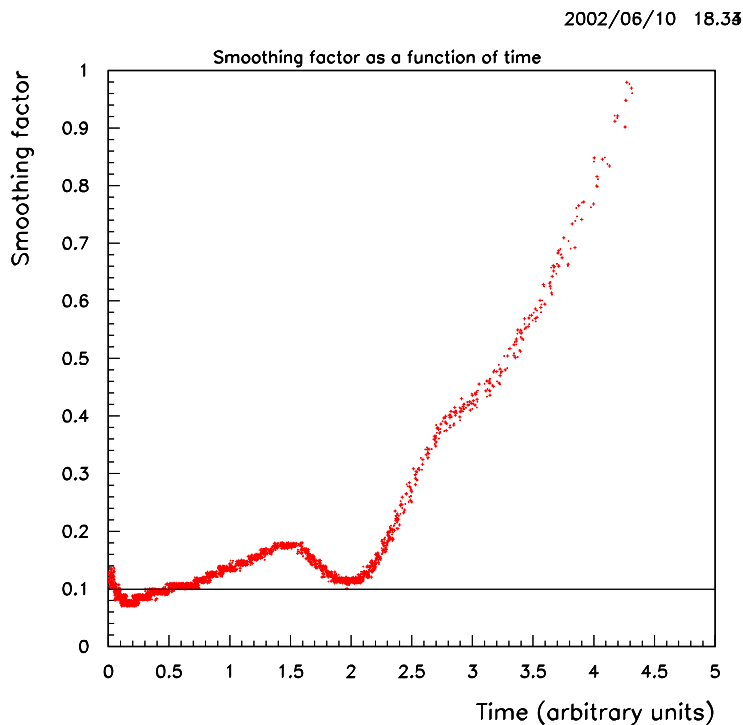


Fig. 3. The variation of  $h$  as a function of  $c$  for the example shown in Figure 5. The variation of the smoothing parameter is obtained iteratively as explained in the text. The flat curve is a smoothing factor resulting from the formula  $h \approx 0.5n^{-1/(d+4)}$ .



### 5.3 An Empirical Measure of the Goodness of Fit

The negative log-likelihood ratio  $\mathcal{NLLR} \equiv -\log_e \mathcal{L}_{\mathcal{R}}$  at the maximum likelihood point now provides a measure of the goodness of fit. In order to use this effectively, one needs an analytic theory of the sampling distribution of this ratio. This is difficult to arrive at, since this distribution is sensitive to the smoothing function used. If adequate smoothing is absent in the tail of the exponential, larger and broader sampling distributions of  $\mathcal{NLLR}$  will result. One can however determine the distribution of  $\mathcal{NLLR}$  empirically, by generating the events distributed according to the theoretical model many times and determining  $\mathcal{NLLR}$  at the maximum likelihood point for each such distribution. The solid histogram in figure 4 shows the distribution of  $\mathcal{NLLR}$  for 500 such fits. This has a mean of 2.8 and an *rms* of 1.8. The dotted histogram shows the corresponding value of  $\mathcal{NLLR}$  for the constant value of smoothing factor shown in figure 3. This distribution is clearly broader (*rms*=2.63) with a higher mean(=9.1) and thus has less discrimination power in judging the goodness of fit than the solid curve.

With this modification in the *PDE*, one gets a good description of the behavior of the data by the *PDE* as shown in Figure 5. We now vary the number of events in the Gaussian and obtain the value of the negative log likelihood ratio  $\mathcal{NLLR}$  as a function of the strength of the Gaussian. Table 1 summarizes the results. The number of standard deviations the unbinned likelihood fit is from what is expected is determined empirically by plotting the value of  $\mathcal{NLLR}$  for a large number of fits where no Gaussian is superimposed (i.e. the null hypothesis) and determining the mean and *RMS* of this distribution and using these to estimate the number of  $\sigma$ 's the observed  $\mathcal{NLLR}$  is from the

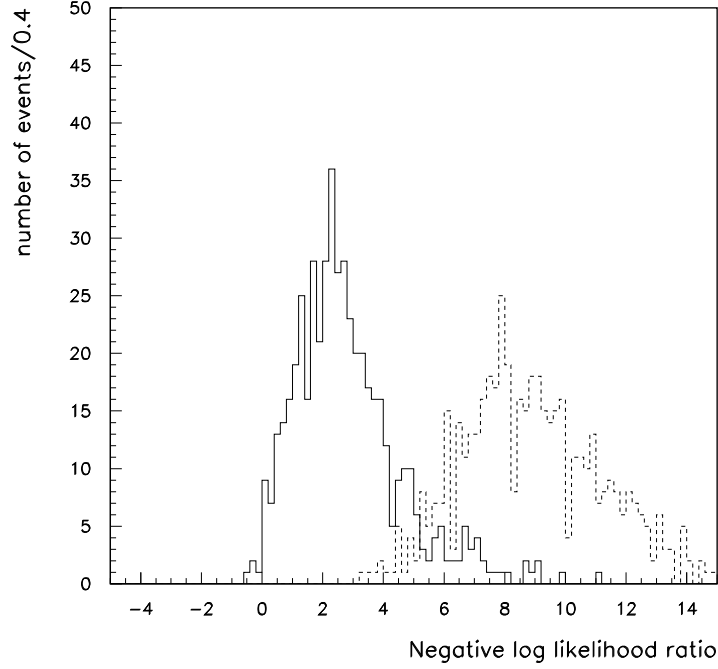


Fig. 4. The solid curve shows the distribution of the negative log likelihood ratio  $\mathcal{NLLR}$  at the maximum likelihood point for 500 distributions, using the iterative smoothing function mechanism. The dashed curve shows the corresponding distribution in the case of a constant smoothing function.

null case. Table 1 also gives the results of a binned fit on the same “data”. It can be seen that the unbinned fit gives a  $3\sigma$  discrimination when the number of Gaussian events is 85, where as the binned fit gives a  $\chi^2/ndf$  of 42/39 for the same case.

Figure 6 shows the variation of  $-\log P(\vec{c}_n|s)$  and  $-\log P^{PDE}(\vec{c}_n)$  for an ensemble of 500 experiments each with the number of events  $n = 1000$  in the exponential and no events in the Gaussian (null hypothesis). One notes that  $-\log P(\vec{c}_n|s)$  and  $-\log P^{PDE}(\vec{c}_n)$  are correlated with each other and the difference between the two ( $-\log \mathcal{NLLR}$ ) is a much narrower distribution than either and provides the goodness of fit discrimination.

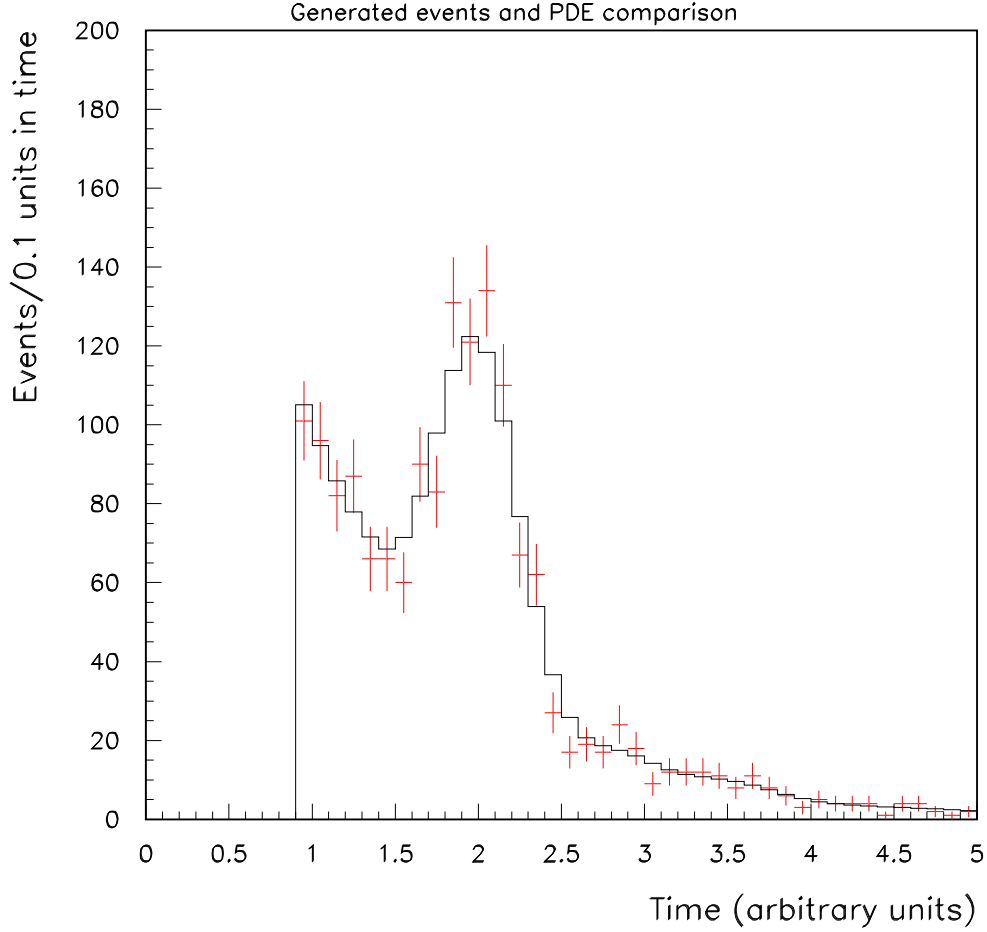


Fig. 5. Figure shows the histogram (with errors) of 1000 events in the fiducial interval  $1.0 < c < 5.0$  generated as an exponential with decay constant  $s=1.0$  with a superimposed Gaussian of 500 events centered at  $c=2.0$  and width=0.2. The *PDE* estimator is the (solid) histogram with no errors.

#### 5.4 Improving the *PDE*

The *PDE* technique we have used so far suffers from two drawbacks; firstly, the smoothing parameter has to be iteratively adjusted significantly over the full range of the variable  $c$ , since the distribution  $P(c|s)$  changes significantly over that range; and secondly, there are boundary effects at  $c=0$  as shown in

Table 1

Goodness of fit results from unbinned likelihood and binned likelihood fits for various data samples. The negative values for the number of standard deviations in some of the examples is due to statistical fluctuation.

Number of Gaussian events	Unbinned fit $\mathcal{NLLR}$	Unbinned fit $N\sigma$	Binned fit $\chi^2$ 39 d.o.f.
500	189.	103	304
250	58.6	31	125
100	11.6	4.9	48
85	8.2	3.0	42
75	6.3	1.9	38
50	2.55	-0.14	30
0	0.44	-1.33	24

figure 2. Both these flaws are remedied if we define the  $PDE$  in hypercube space. After we find the maximum likelihood point  $s^*$ , for which the  $PDE$  is not needed, we transform the variable  $c \rightarrow c'$ , such that the distribution  $P(c'|s^*)$  is flat and  $0 < c' < 1$ . The hypercube transformation can be made even if  $c$  is multi-dimensional by initially going to a set of variables that are uncorrelated and then making the hypercube transformation. The transformation can be such that any interval in  $c$  space maps on to the interval  $(0, 1)$  in hypercube space.

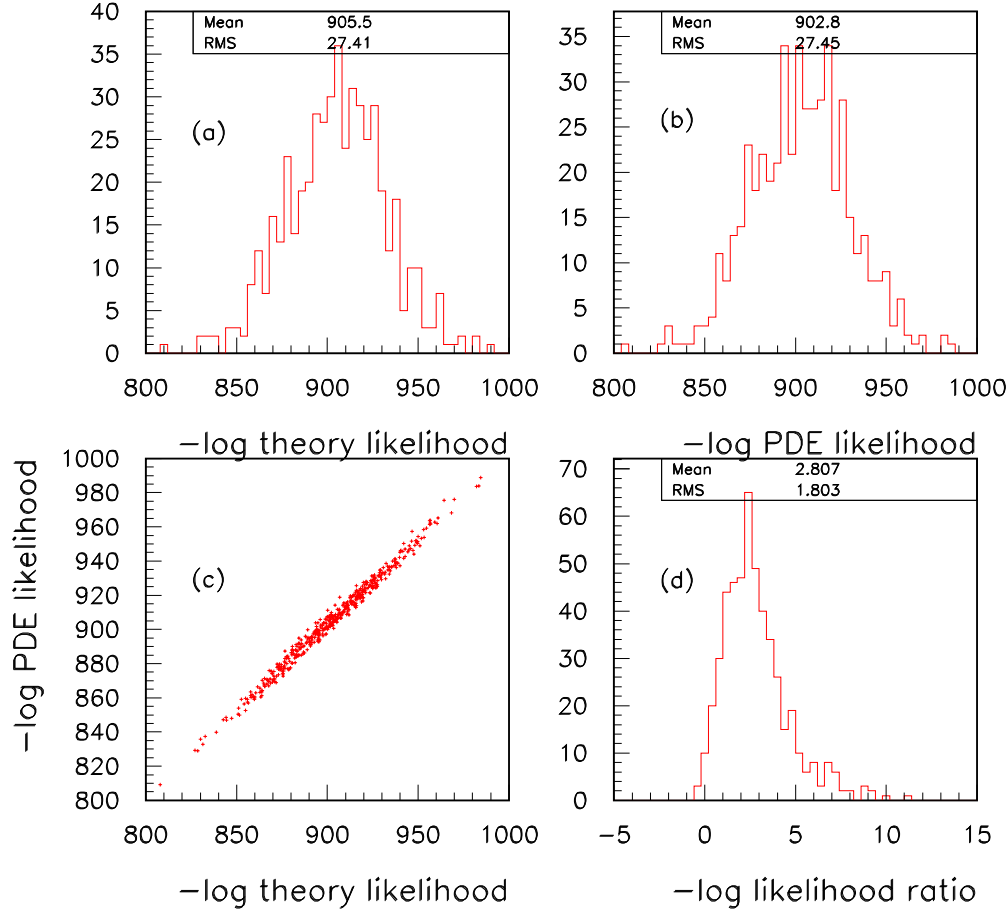


Fig. 6. (a) shows the distribution of the negative log-likelihood  $-\log_e(P(\vec{c}_n|s))$  for an ensemble of experiments where data and experiment are expected to fit. (b) Shows the negative log  $PDE$  likelihood  $-\log_e(P(\vec{c}_n))$  for the same data (c) Shows the correlation between the two and (d) Shows the negative log-likelihood ratio  $\mathcal{NLLR}$  that is obtained by subtracting (b) from (a) on an event by event basis.

### 5.5 Periodic Boundary Conditions

We solve the boundary problem by imposing periodicity in the hypercube. In the one dimensional case, we imagine three “hypercubes”, each identical to the other on the real axis in the intervals  $(-1, 0)$ ,  $(0, 1)$  and  $(1, 2)$ . The

hypercube of interest is the one in the interval  $(0, 1)$ . When the probability from an event kernel leaks outside the boundary  $(0, 1)$ , we continue the kernel to the next hypercube. Since the hypercubes are identical, this implies the kernel re-appearing in the middle hypercube but from the opposite boundary. Put mathematically, the kernel is defined such that

$$\mathcal{G}(c' - c'_i) = \mathcal{G}(c' - c'_i - 1); c' > 1 \quad (59)$$

$$\mathcal{G}(c' - c'_i) = \mathcal{G}(c' - c'_i + 1); c' < 0 \quad (60)$$

Although a Gaussian Kernel will work on the hypercube, the natural kernel to use considering the shape of the distribution in hypercube space (it is flat for a good fit), would be the “boxcar function”  $\mathcal{G}(c')$ .

$$\mathcal{G}(c') = \frac{1}{h}; |c'| < \frac{h}{2} \quad (61)$$

$$\mathcal{G}(c') = 0; |c'| > \frac{h}{2} \quad (62)$$

This kernel would be subject to the periodic boundary conditions given above, which further ensure that every configuration in hypercube space is treated exactly as every other configuration irrespective of its co-ordinate. The parameter  $h$  is a smoothing parameter which needs to be chosen with some care. However, since the theory distribution is flat in hypercube space, the smoothing parameter may not need to be iteratively determined over hypercube space to the extent that data distribution is similar to the theory distribution. Even if iteration is used, the variation in  $h$  in hypercube space is likely to be much smaller.

Figure 7 shows the distribution of the  $\mathcal{NLLR}$  for the null hypothesis for an ensemble of 500 experiments each with 1000 events as a function of the smoothing factor  $h$ . It can be seen that the distribution narrows considerably

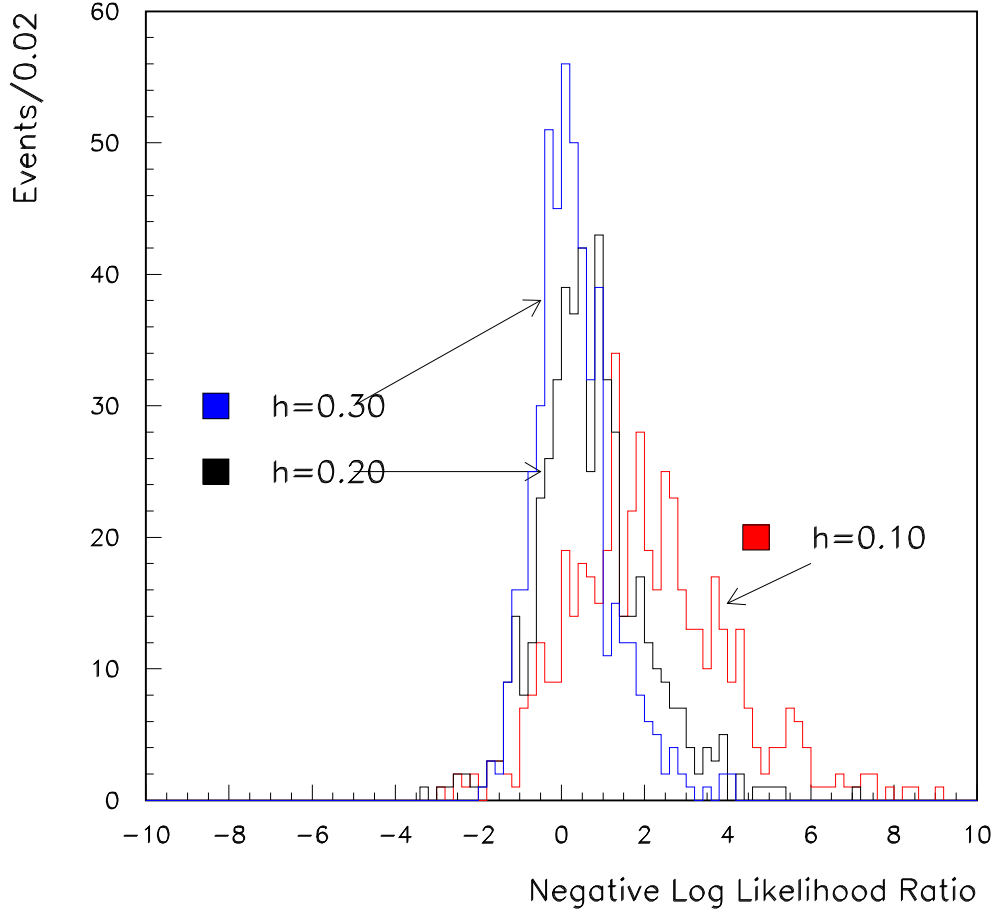


Fig. 7. The distribution of the negative log likelihood ratio  $\mathcal{NLLR}$  for the null hypothesis for an ensemble of 500 experiments each with 1000 events, as a function of the smoothing factor  $h=0.1, 0.2$  and  $0.3$

as the smoothing factor increases. We choose an operating value of  $0.2$  for  $h$  and study the dependence of the  $\mathcal{NLLR}$  as a function of the number of events ranging from  $100$  to  $1000$  events, as shown in figure 8. The dependence on the number of events is seen to be weak, indicating good behavior. The *PDE* thus arrived computed with  $h=0.2$  can be transformed from the hypercube space to  $c$  space and will reproduce data smoothly and with no edge effects. We note that it is also easier to arrive at an analytic theory of  $\mathcal{NLLR}$  with the choice

of this simple kernel.

2003/11/28 19.51

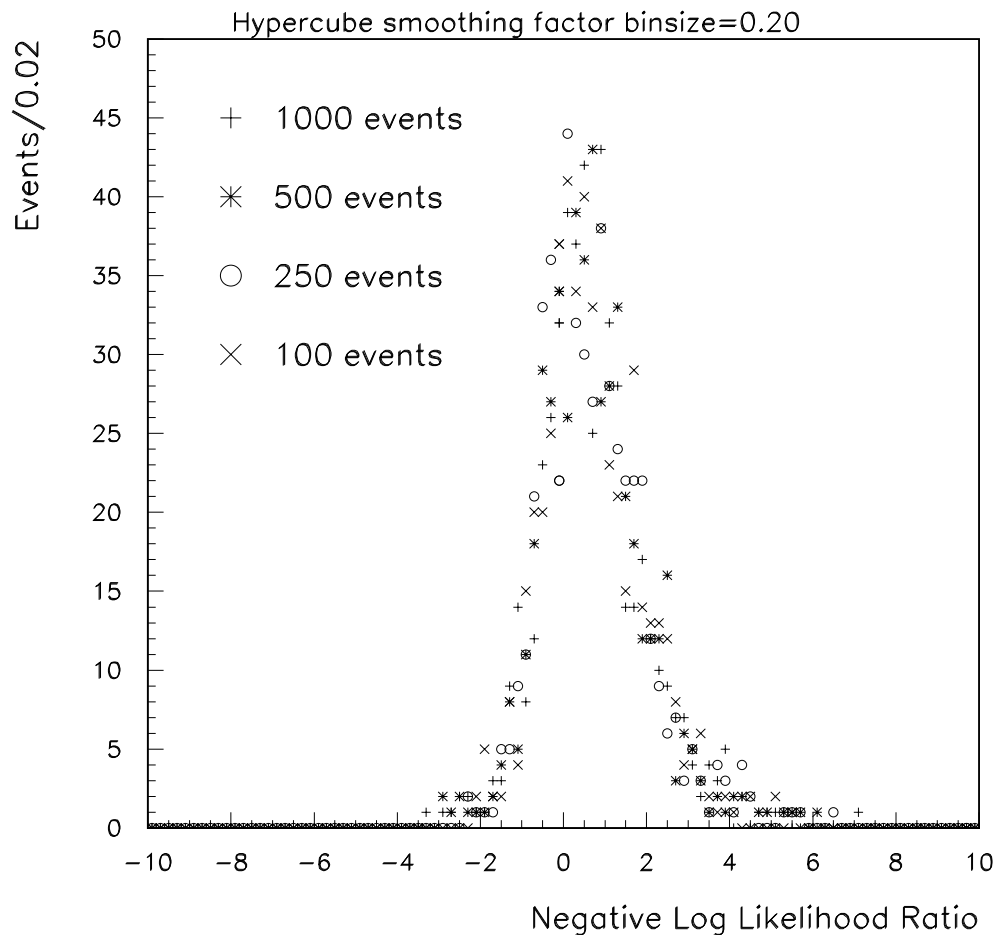


Fig. 8. The distribution of the negative log likelihood ratio  $\mathcal{NLLR}$  for the null hypothesis for an ensemble of 500 experiments each with the smoothing factor  $h=0.2$ , as a function of the number of events

## 6 The distribution of the goodness of fit variable

Of all the goodness of fit variables we have studied above, for both binned and unbinned likelihood fits, the  $\chi^2$  variable is the most studied and has an



analytic theory associated with its distribution. This is used to set a  $p$ -value for the goodness of fit, defined as the probability to exceed the observed value  $\chi^2$  based on its analytic distribution. In the absence of an analytic theory, it is possible to use Monte Carlo methods to obtain the distribution of the goodness of fit variable for the hypothesis being tested and to numerically obtain the  $p$ -value.

## 7 Calculation of fitted errors

After the fitting is done and the goodness of fit is evaluated, one needs to work out the errors on the fitted quantities. One needs to calculate the probability density  $P(s|\vec{c}_n)$ , which carries information not only about the maximum likelihood point  $s^*$ , from a single experiment, but how such a measurement is likely to fluctuate if we repeat the experiment. This problem is known as the “problem of inverse probabilities” in statistical literature and is solved by the use of Bayes’ theorem. Since Bayes’ theorem is central to the arguments that follow, we give a simple derivation of it here.

### 7.1 Derivation of Bayes’ theorem equations

Consider a joint probability distribution  $P(s, c)$  in variables  $s, c$ . For the sake of simplicity, we will take both  $s$  and  $c$  to be one-dimensional. The arguments being made are general enough to easily change them into multi-dimensional variables. Figure 9 shows geometrically the two dimensional space of  $s$  and  $c$ . We plot  $s$  as the ordinate and  $c$  as the abscissa. At this stage  $s$  and  $c$  are two

general variables. Then,

$$\int \int P(s, c) ds dc = 1 \quad (63)$$

We define the single variable probabilities  $P(c)$  and  $P(s)$  as

$$P(c) = \int P(s, c) ds \quad (64)$$

$$P(s) = \int P(s, c) dc \quad (65)$$

$P(c)$  is the probability density of  $c$  irrespective of the value of  $s$  and  $P(s)$  is the probability density of  $s$  irrespective of the value of  $c$ . It follows from equation 63 that

$$\int P(s) ds = 1 \quad (66)$$

and

$$\int P(c) dc = 1 \quad (67)$$

We define a conditional probability  $P(c|s)$  as the probability of observing  $c$  given  $s$ . It is thus, the joint probability  $P(s, c)$  along the slice AB ( $s=\text{constant}$ ) in figure 9, appropriately normalized to unity. *i.e.*,

$$P(c|s) = \frac{P(s, c)}{\int P(s, c) dc} \quad (68)$$

where the denominator in the above equation ensures that  $\int P(c|s) dc = 1$ .

Therefore, (using equation 65)

$$P(c|s) = \frac{P(s, c)}{P(s)} \quad (69)$$

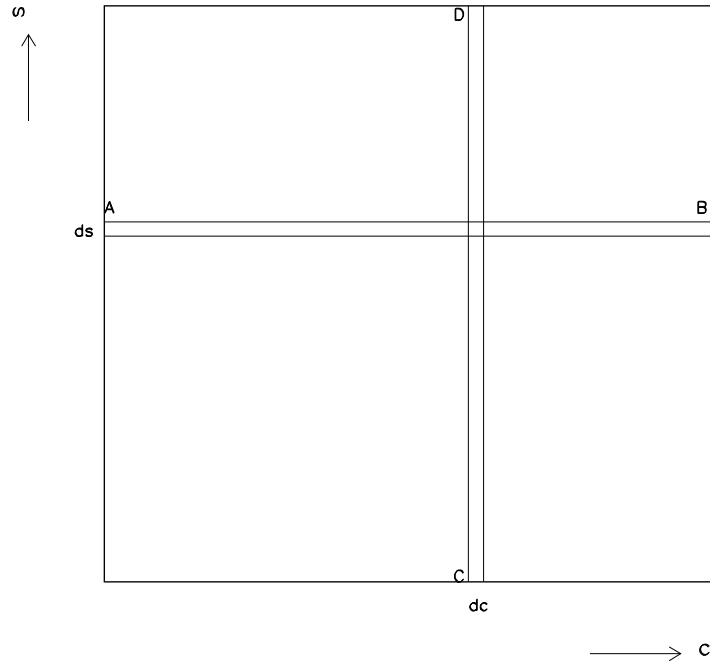


Fig. 9. Joint probability distribution in the variables  $s$ ,  $c$ . Conditional probabilities are computed along the slices AB ( $s=\text{constant}$ ) and CD ( $c=\text{constant}$ ).

By symmetrical arguments (integrations along the slice CD), we show that the conditional probability  $P(s|c)$  is given by

$$P(s|c) = \frac{P(s, c)}{P(c)} \quad (70)$$

leading to the joint probability equation

$$P(s, c) = P(c|s)P(s) = P(s|c)P(c) \quad (71)$$

which is sometimes written in a more familiar form known as Bayes' theorem [7] as

$$P(s|c) = \frac{P(c|s)P(s)}{P(c)} \quad (72)$$

By substituting the expression for  $P(s, c)$  in equation 69 in equation 64 we get the equation

$$P(c) = \int P(c|s)P(s)ds \quad (73)$$

and by substituting the expression for  $P(s, c)$  in equation 70 in equation 65 we get the equation

$$P(s) = \int P(s|c)P(c)dc \quad (74)$$

These complete the Bayes' theorem equations. Note also that the joint probability equation 71 can be written in a form a likelihood ratio  $\mathcal{L}_R$

$$\mathcal{L}_R = \frac{P(s|c)}{P(s)} = \frac{P(c|s)}{P(c)} \quad (75)$$

The quantity  $\mathcal{L}_R$  equation 75 is invariant under change of variables  $c \rightarrow c'$  and  $s \rightarrow s'$ , since the Jacobian of the transformation  $|\frac{\partial c'}{\partial c}|$  divides out in the numerator and the denominator for the right hand side of the equation 75 for the ratio of probability densities in  $\frac{P(c|s)}{P(c)}$ . Similarly the ratio is invariant under the transformation variable  $s$  in the LHS of the equation. These invariances are essential in the use of the ratio  $\mathcal{L}_R$  as a goodness-of-fit variable.

We can then extend the derivation given above to derive Bayes' theorem equations for the dataset  $\vec{c}_n$ .

$$P(s, \vec{c}_n) = P(\vec{c}_n|s)P(s) = P(s|\vec{c}_n)P(\vec{c}_n) \quad (76)$$

$$P(\vec{c}_n) = \int P(\vec{c}_n|s)P(s)ds \quad (77)$$

$$P(s) = \int P(s|\vec{c}_n)P(\vec{c}_n)d\vec{c}_n \quad (78)$$

Let us note that Bayes' theorem as derived above is a theorem in mathematics that applies to any integrable function of two variables  $P'(s, c)$  for which the normalized function  $P(s, c) = \frac{P'(s, c)}{\iint P'(s, c) ds dc}$  can be constructed. The “probabilities”  $P(s)$  and  $P(c)$  are projections of such a function and the “conditional probabilities”  $P(c|s)$  and  $P(s|c)$  are normalized slices of such a function. How we identify the slices and projections to correspond to probability theory is up to us. Once the joint probability function  $P(s, c)$  can be specified, the inverse probability problem can be solved, since the inverse probability is given by the slice  $P(s|c)$  and the theoretical likelihood is given by the slice  $P(c|s)$ . In order to specify the joint probability, the Bayesians specify the theoretical likelihood  $P(\vec{c}_n|s)$  and the projection on the parameter axis  $P(s)$  which they term the Bayesian prior. We now describe the Bayesian paradigm and the difficulties associated with it.

## 7.2 The Bayesian Paradigm

The theoretical likelihood  $P(\vec{c}_n|s)$  is specified by the model in question. In order to specify the joint probability, Bayesians supply the function  $P(s)$ , which they term the Bayesian prior. The joint probability is then given by

$$P(s, \vec{c}_n) = P(\vec{c}_n|s)P(s) = P(s|\vec{c}_n)P(\vec{c}_n) \quad (79)$$

and the inverse probability is obtained by

$$P(s|\vec{c}_n) = \frac{P(\vec{c}_n|s)P(s)}{P(\vec{c}_n)} = \frac{P(\vec{c}_n|s)P(s)}{\int P(\vec{c}_n|s)P(s)ds} \quad (80)$$

The Bayesian prior  $P(s)$  is an unknown function that according to the Bayesians encapsulates the prior knowledge the experimenter has on the true value of the

parameter. There exists many different methods of estimating the unknown prior. We briefly describe them here.

### 7.2.1 *Objective Bayesianism*

In this sub-branch of Bayesianism, the prior is assumed to be known within some limits that the user supplies and the distribution is assumed to be flat within those limits. This approach is championed by statisticians such as Jaynes [9]. If one specifies a flat prior in a variable  $s$ , then it is clearly not a flat prior in a transformed variable  $s' = s'(s)$ . The maximum likelihood analysis can be carried out in any function  $s'(s)$  and the maximum likelihood point  $s^*$  would be the same under such transformations, i.e.

$$s^{*'} = s'(s^*) \tag{81}$$

However, if a flat Bayesian prior is assumed in one variable, it would not be flat in any function of that variable. The results would depend on the prior assumed. This is a serious objection to this method.

### 7.2.2 *Subjective Bayesianism*

This approach is championed by statisticians such as de Finetti [10] where the experimenter specifies the prior based on “subjective criteria” based on his past experience and knowledge of the parameter  $s$ . If more than one experimenter is involved, then more than one prior can be used and more than one posterior density results.

### 7.2.3 Hierarchical Bayesianism

This sub-branch of Bayesianism attempts to parametrize the prior [11] in terms of more unknown parameters each of which have their own priors, forming a hierarchy.

### 7.2.4 Empirical Bayesianism

Empirical Bayesianism [12] attempts to stem the infinite hierarchy of priors implied by hierarchical Bayesianism by attempting to determine some of the parameters associated with the priors from the data.

Note all Bayesians [13] treat the projection  $P(\vec{c}_n)$  as an uninteresting constant of normalization, theoretically obtained by the equation

$$P(\vec{c}_n) = \int P(\vec{c}_n|s)P(s)ds \quad (82)$$

whose right hand side consists of an integral over the Bayesian prior and the theoretical likelihood. However, having solved the goodness of fit problem, we have demonstrated that the data likelihood  $P^{data}(\vec{c}_n)$  carries with it vital information relevant for goodness of fit. It may be thought of as the *pdf* of the  $n - object$   $\vec{c}_n$  and must be empirically determined from experimental data. If we use this function from the data as a projection of the joint probability and the theoretical likelihood  $P(\vec{c}_n|s)$  as a slice, then we can invert the probability to obtain  $P(s|\vec{c}_n)$  without the use of a Bayesian prior. What results is a new paradigm in statistics where we have to re-define some concepts to be consistent with this interpretation.

### 7.3 The New Paradigm

We note that if we identify the projection  $P(\vec{c}_n)$  of the joint probability  $P(s, \vec{c}_n)$  as the data-likelihood, which we denote  $P^{data}(\vec{c}_n)$ , then the projection on the  $s$  axis depends on  $n$  and is thus incompatible with being a Bayesian prior that is independent of  $n$ .

To show this, let us note that the inverse probability  $P(s|\vec{c}_n) \rightarrow \delta(s - s_T)$  as  $n \rightarrow \infty$  where  $s_T$  is the true value of  $s$ . This is a result of the central limit theorem of statistics and contains the assumption that the experiment is unbiased. Then, using equation 78 and  $P^{data}(\vec{c}_n)$  for one of the projections, one obtains

$$P(s) = \int P(s|\vec{c}_n) P^{data}(\vec{c}_n) d\vec{c}_n \quad (83)$$

But,  $P^{data}(\vec{c}_n) d\vec{c}_n$  represents the probability of obtaining the dataset  $\vec{c}_n$  in the neighborhood of the dataset  $\vec{c}_n$ . If one were to repeat the experiment  $N$  times, thus obtaining an ensemble of datasets, then  $P^{data}(\vec{c}_n) d\vec{c}_n = \frac{dN}{N}$  for  $N \rightarrow \infty$ . Then,

$$P(s) = \int P(s|\vec{c}_n) \frac{dN}{N} = \frac{1}{N} \sum_{k=1}^{k=N} P_k(s|\vec{c}_n) = \langle P(s|\vec{c}_n) \rangle \quad (84)$$

where  $k$  denotes the ensemble member and the symbols  $\langle \rangle$  represent average over the ensemble of the function. However, since  $P_k(s|\vec{c}_n) \rightarrow \delta(s - s_T)$ , as  $n \rightarrow \infty$ , we would expect  $P(s) \rightarrow \delta(s - s_T)$  in this limit. i.e.  $P(s)$  cannot find interpretation as an  $n$ -independent Bayesian prior. We note however, that if one were to plot the probability distribution of the maximum likelihood value  $s^*$  of each member of the ensemble, then such a distribution would have



the desired  $n$  dependence, becoming narrower for larger  $n$ . We thus build our theory by identifying the projection on the parameter axis as the probability distribution of  $s^*$ , which we denote by  $\mathcal{P}_n(s^*)$ , explicitly indicating the  $n$  dependence. Then the joint probability distribution  $P(s^*, \vec{c}_n)$  is given by

$$P(s^*, \vec{c}_n) = P(\vec{c}_n | s^*) \mathcal{P}_n(s^*) \quad (85)$$

Each member  $k$  of the ensemble has a maximum likelihood value  $s_k^*$ . The probability distribution of this quantity over an infinite ensemble is defined to be  $\mathcal{P}_n(s^*)$ . This definition is similar in spirit to the “fiducial probability” of R. A. Fisher [14]. We are now able to specify the joint probability  $P(s^*, \vec{c}_n)$  as per equation 85. Then by Bayes’ theorem, we can also write

$$P(s^*, \vec{c}_n) = P(s^* | \vec{c}_n) P^{data}(\vec{c}_n) = P(\vec{c}_n | s^*) \mathcal{P}_n(s^*) \quad (86)$$

where this equation is the definition of the inverse probability  $P(s^* | \vec{c}_n)$ . This implies that from the  $k^{th}$  element of the ensemble, consisting of a single dataset  $\vec{c}_n$ , not only is the maximum likelihood value  $s_k^*$  available, but also information on the distribution of  $s^*$  from other similar datasets on the ensemble. It is the availability of this information that permits the estimation of errors based on one dataset. This then leads to the solution of the inverse probability on the ensemble by the usual Bayes’ theorem equation.

$$P(s^* | \vec{c}_n) = \frac{P(\vec{c}_n | s^*) \mathcal{P}_n(s^*)}{P^{data}(\vec{c}_n)} = \frac{P(\vec{c}_n | s^*) \mathcal{P}_n(s^*)}{\int P(\vec{c}_n | s^{*'}) \mathcal{P}_n(s^{*'}) ds^{*'}} \quad (87)$$

Equation 87 shows us how to obtain the inverse probability  $P(s^* | \vec{c}_n)$  once we have the ensemble and hence is not much use to us, since it requires an infinite number of similar experiments on the ensemble. Our problem is to obtain the inverse probability given a single member of the ensemble. Before we proceed

to solve this problem, let us note that on the ensemble, Bayes' theorem is expressed in the following elegant set of equations.

$$\mathcal{P}_n(s^*) = \int P(s^*|\vec{c}_n)P^{data}(\vec{c}_n)d\vec{c}_n = \langle P(s^*|\vec{c}_n) \rangle \quad (88)$$

$$\mathcal{P}(\vec{c}_n) = \int P(\vec{c}_n|s^*)\mathcal{P}_n(s^*)ds^* = \langle P(\vec{c}_n|s^*) \rangle \quad (89)$$

$$\mathcal{L}_R^k(s^*) = \frac{P_k(s^*|\vec{c}_n)}{\langle P(s^*|\vec{c}_n) \rangle} = \frac{P_k(\vec{c}_n|s^*)}{\langle P(\vec{c}_n|s^*) \rangle} \quad (90)$$

In the above set of equations, we have used the symbol  $\mathcal{P}(\vec{c}_n)$  to denote the data *pdf* determined on an infinite ensemble to distinguish it from  $P_k^{data}(\vec{c}_n)$  which is the data pdf determined from a single member of the ensemble. The former benefits from the statistics present in the infinite ensemble. Equation 90 gives the the likelihood ratio on the ensemble of each member of the ensemble that may be used for goodness of fit once the ensemble is known. Note that there is no Bayesian prior used anywhere in the above set of equations.

### 7.3.1 The true value of the parameter $s$

The true value  $s_T$  of the parameter  $s$  is defined to be that value of  $s^*$  at which the maximum of the *pdf*  $\mathcal{P}_n(s^*)$  occurs. Let us remember that  $\mathcal{P}_n(s^*)$  has an infinite number of similar datasets  $\vec{c}_n$  contributing to it and hence this is just a statement of the experiments being unbiased. The true value is a number. It does not possess a distribution.

### 7.3.2 The unknowability of $\mathcal{P}_n(s^*)$

Since the true value  $s_T$  can never be determined to infinite precision, and the true value is the abscissa for which the *pdf*  $\mathcal{P}_n(s^*)$  is the maximum, it follows that the function  $\mathcal{P}_n(s^*)$  is unknowable. We cannot associate an abscissa to the

function  $\mathcal{P}_n(s^*)$  and hence the function cannot be “anchored” to the  $s^*$  axis. If we could anchor it, we could read off the value of  $s_T$  to infinite precision by determining the maximum likelihood value of the function. We thus term this function an “unknown concomitant”, to distinguish it from a Bayesian prior. It is an abstraction which we approach with ever increasing precision as we increase  $N$ , the number of members on the ensemble.

### 7.3.3 The standard error on the fitted parameter

The function  $\mathcal{P}_n(s^*)$  is the probability distribution of the maximum likelihood values  $s_k^*$  on the ensemble. The standard error  $\sigma_n$  of the fitted parameter is defined as

$$\sigma_n^2 = \int (s^* - s_T)^2 \mathcal{P}_n(s^*) ds^* = \langle (s^* - s_T)^2 \rangle \quad (91)$$

We also note that  $\mathcal{P}_n(s^*) = \langle P(s^* | \vec{c}_n) \rangle$  is *also* the ensemble average of the inverse probability functions  $P_k(s^* | \vec{c}_n)$ . Hence the inverse probability function  $P_k(s^* | \vec{c}_n)$  from a single dataset  $k$  is an unbiased estimator of the (unknowable) function  $\mathcal{P}_n(s^*)$  and its variance can be used to estimate the standard error  $\sigma_n$ .

### 7.3.4 The evaluation of the inverse probability $P_k(s^* | \vec{c}_n)$ : The error bootstrap

We now need to compute the function  $P_k(s^* | \vec{c}_n)$ . We employ Bayes’ theorem to do this. The error on the fitted parameter  $s^*$  will be related to the width of the inverse probability  $P_k(s^* | \vec{c}_n)$  that we are trying to compute. It is also related to our ignorance of the value of  $s_T$  and our inability to anchor the distribution  $\mathcal{P}_n(s^*)$ . Our level of ignorance of where to anchor the distribution  $\mathcal{P}_n(s^*)$  is

directly related to the error we are trying to compute and is directly related to the width of  $P_k(s^*|\vec{c}_n)$ . At this stage, we have worked out the likelihood ratio  $\mathcal{L}_{\mathcal{R}}^k(s)$  as a function of  $s$  and have evaluated the maximum likelihood value  $s_k^*$ . The argument  $s$  of the likelihood ratio is a dummy argument of a function and we are at liberty to change it to the argument  $s^*$  as in  $\mathcal{L}_{\mathcal{R}}^k(s^*)$  for further discussion. We can choose an arbitrary value of  $s^*$  and evaluate the goodness of fit at that value using the likelihood ratio. When we do this, we are in fact hypothesizing that  $s_T$ , the true value, is at this value of  $s^*$ . The function  $\mathcal{L}_R(s^*)$  then gives us a way of evaluating the goodness of fit of the hypothesis as we change  $s^*$ . Let us now take an arbitrary value of  $s^*$  and hypothesize that that is the true value. Then, consistent with our hypothesis, we must insist that the distribution  $\mathcal{P}_n(s^*)$  is moved so that the maximum value of the distribution (i.e.  $s_T$ ) is at the current value of  $s^*$ .

At the true value  $s_T$ , the Bayes' theorem equations for the joint probability state

$$P(s_T, \vec{c}_n) = P(\vec{c}_n|s_T)\mathcal{P}_n(s_T) = P(s_T|\vec{c}_n)P^{data}(\vec{c}_n) \quad (92)$$

We now hypothesize that the true value is at  $s^* = s_1$ . Then the above equation will read

$$P(s_1, \vec{c}_n) = P(\vec{c}_n|s_1)\mathcal{P}_n(s_T) = P(s_1|\vec{c}_n)P^{data}(\vec{c}_n) \quad (93)$$

When we change the hypothesis to a different value  $s^* = s_2$ , then the equation will read

$$P(s_2, \vec{c}_n) = P(\vec{c}_n|s_2)\mathcal{P}_n(s_T) = P(s_2|\vec{c}_n)P^{data}(\vec{c}_n) \quad (94)$$

We have moved the distribution  $\mathcal{P}_n(s^*)$  to accommodate our changing hypothesis from the true value being at  $s_1$  to  $s_2$ . These hypotheses are mutually exclusive in that the true value cannot be at both  $s_1$  and  $s_2$ . This mandates that we move the function  $\mathcal{P}_n(s^*)$  as we change the hypothesis. This set of hypotheses thus communicate to our system of equations, our ignorance of the position of the true value. The set of hypotheses form an OR of the position of the true value, whereas by contrast, the Bayesian prior expresses an AND of the position of the true value. Then for the hypothesis that the true value is at an arbitrary  $s^*$ , the above equations become

$$P(s^*, \vec{c}_n) = P(\vec{c}_n | s^*) \mathcal{P}_n(s_T) = P(s^* | \vec{c}_n) P^{data}(\vec{c}_n) \quad (95)$$

Re-arranging,

$$P(s^* | \vec{c}_n) = \frac{P(\vec{c}_n | s^*)}{P^{data}(\vec{c}_n)} \mathcal{P}_n(s_T) \quad (96)$$

Imposing the normalization condition  $\int P(s^* | \vec{c}_n) ds^* = 1$  yields

$$P_k(s^* | \vec{c}_n) = \frac{P_k(\vec{c}_n | s^*)}{\int P_k(\vec{c}_n | s^{*'}) ds^{*'}} \quad (97)$$

where we have explicitly indicated the dependence on the ensemble index  $k$ . To reiterate, when one varies  $s^*$  in equation 95, one makes the hypothesis that  $s = s_T$ . As one changes  $s^*$ , a new hypothesis is being tested that is mutually exclusive from the previous one, since the true value can only be at one location. So as one changes  $s^*$ , one is compelled to move the *distribution*  $\mathcal{P}_n(s^*)$  so that  $s_T$  is at the value of  $s^*$  being tested. *If one did not move  $\mathcal{P}_n(s^*)$ , then this is tantamount to anchoring the function to the  $s^*$  axis and this is not allowable, since the true value is unknown.* This implies that  $\mathcal{P}_n(s_T)$  does not change as one changes  $s^*$  and is a constant *wrt*  $s^*$ . Figure 10 illustrates

these points graphically. Thus  $\mathcal{P}_n(s_T)$  in our equations is a number, not a function. We have thus “bootstrapped” the error. On the one hand,  $P_k(s^*|\vec{c}_n)$  gives us an estimate of the spread in the measurements of  $s^*$  from an ensemble of datasets  $\vec{c}_n$ , based on one such data set. On the other hand, the error in  $s^*$  is expressed in the uncertainty on where to put  $s_T$ . We have connected these two uncertainties using Bayes’ theorem and hypothesis testing. Also,

$$\mathcal{P}_n(s_T) = \frac{1}{\int \mathcal{L}_R(s^*)ds^*} = \frac{P^{data}(\vec{c}_n)}{\int P(\vec{c}_n|s^*)ds^*} \quad (98)$$

We have thus determined  $\mathcal{P}_n(s_T)$ , the value of the “unknown concomitant” at the true value  $s_T$  using our data set  $c_n$ . This is our *measurement* of  $\mathcal{P}_n(s_T)$  and different datasets will give different values of  $\mathcal{P}_n(s_T)$ , in other words  $\mathcal{P}_n(s_T)$  will have a sampling distribution with an expectation value and standard deviation.

Note that it is only possible to write down an expression for  $\mathcal{P}_n(s_T)$  dimensionally when a likelihood ratio  $\mathcal{L}_R$  is available. The equation 97 is the same expression that “frequentists” use for calculating their errors after fitting, namely the likelihood curve normalized to unity gives the parameter errors. If the likelihood curve is Gaussian shaped, then this justifies a change of negative log-likelihood of  $\frac{1}{2}$  from the maximum likelihood point to get the  $1\sigma$  errors. Similarly, when performing  $\chi^2$  fitting, it is now rigorously permitted to use  $\Delta\chi^2 = 1$  to estimate errors in fitted parameters under the Gaussian assumption. No Bayesian prior is needed.

The “Objective Bayesians” may be tempted to remark that equation 97 is the same equation they would derive using a flat prior and so the two theories are equivalent. This is not the case, since their projection of the joint probability

on the parameter axis is the Bayesian prior which does not depend on  $n$  (for all Bayesians), whereas in our case it yields a function  $\mathcal{P}_n(s^*)$  which depends on  $n$ . So the two theories are radically different. Also, in the new paradigm, one does not have to answer the question “Flat in what variable?”, as the “Objective Bayesians” have to do regarding the prior they use. Our theory is invariant no matter what the density of the hypotheses we make in  $s^*$  space is. The Bayesians will obtain different results when they use different densities for the prior distribution.

### 7.3.5 *Iterative behavior of the theory when more than one member of the ensemble is available*

We have now solved the problem for the case when one member of the ensemble is available. This is what happens in most cases, when only one dataset exists. If however we want to study the theory when more the one member of the ensemble is present, we can proceed to use equation 88 to work out a better approximation for  $\mathcal{P}_n(s^*)$ .

$$\mathcal{P}_n(s^*) = \langle P(s^*|\vec{c}_n) \rangle \approx \frac{1}{N} \sum_{k=1}^{k=N} P_k(s^*|\vec{c}_n) \quad (99)$$

We now have an approximation to the function  $\mathcal{P}_n(s^*)$  which is based on  $N$  datasets instead of one. This approximation can be used to iterate our functions  $P_k(s^*|\vec{c}_n)$  using equation 87.

$$P_k^{(2)}(s^*|\vec{c}_n) = \frac{P_k(\vec{c}_n|s^*)\mathcal{P}_n(s^*)}{\int P_k(\vec{c}_n|s^{*'})\mathcal{P}_n(s^{*'})ds^{*'}} \quad (100)$$

where we have used the superscript (2) to indicate that this is the second iteration of the function. These sets of functions can be used to obtain a new

version of the function  $\mathcal{P}_n(s^*)$  using the relation

$$\mathcal{P}_n^{(2)}(s^*) = \frac{1}{N} \sum_{k=1}^{k=N} P_k^{(2)}(s^*|\vec{c}_n) \quad (101)$$

Similarly, one needs to iterate on the theoretical likelihoods  $P_k(\vec{c}_n|s^*)$  when information from more than one member of the ensemble is available. This is done by using equation 89 to obtain an approximation for  $\mathcal{P}(\vec{c}_n)$ .

$$\mathcal{P}(\vec{c}_n) = \langle P(\vec{c}_n|s^*) \rangle \approx \frac{1}{N} \sum_{k=1}^{k=N} P_k(\vec{c}_n|s^*) \quad (102)$$

This equation states that it is possible to get a better estimate of the density of data  $\mathcal{P}(\vec{c}_n)$  from all the  $N$  members of the ensemble combined than from a single member alone. This is followed by

$$P_k^{(2)}(\vec{c}_n|s^*) = \frac{P_k(s^*|\vec{c}_n)\mathcal{P}(\vec{c}_n)}{\int P_k(s^*|\vec{c}'_n)\mathcal{P}(\vec{c}'_n)d\vec{c}'_n} \quad (103)$$

This equation states that in the presence of all  $N$  members of the ensemble, it is possible to obtain a better value of the likelihood  $P_k(\vec{c}_n|s^*)$  than the theoretical likelihood which assumes that the true value  $s_T$  is at  $s^*$ . The above functions are used to derive an iterated version of the data density  $\mathcal{P}(\vec{c}_n)$  that uses information available from all the members of the ensemble to compute the data density.

$$\mathcal{P}^{(2)}(\vec{c}_n) = \frac{1}{N} \sum_{k=1}^{k=N} P_k^{(2)}(\vec{c}_n|s^*) \quad (104)$$

### 7.3.6 Combining Results of Experiments

Each experiment should publish a likelihood curve for its fit as well as a number for the data likelihood  $P^{data}(\vec{c}_n)$ . Combining the results of two experiments



with  $m$  and  $n$  experiments each, involves multiplying the likelihood ratios.

$$\mathcal{L}_{\mathcal{R}_{m+n}}(s) = \mathcal{L}_{\mathcal{R}_m}(s) \times \mathcal{L}_{\mathcal{R}_n}(s) = \frac{P(\vec{c}_m|s)}{P^{data}(\vec{c}_m)} \times \frac{P(\vec{c}_n|s)}{P^{data}(\vec{c}_n)} \quad (105)$$

Inverted probabilities and goodness of fit can be deduced from the combined likelihood ratio. It is worth noting that the numerator of the likelihood ratio is a function of the fitted parameters and the denominator is a number.

### 7.3.7 Another Illustrative Example

We now apply the theory developed here to a practical example to illustrate the ideas further. The problem is to determine the weight of an object using an apparatus whose standard error is known to be 5 gm. The weight is a fixed constant of nature for the duration of the experiment. We obtain a dataset of 100 measurements, i.e.  $n = 100$ . Then  $P(c|s)$  is a Gaussian of unknown mean  $s$  and width  $\sigma = 5$  gm. We compute  $P(\vec{c}_n|s)$  for the 100 events by multiplying the individual  $P(c_i|s)$  together and maximize the likelihood to determine  $s^*$  for the dataset using unbinned likelihoods. We then transform the measurements  $c_i$  to the hypercube space using equation 3. We use the improved  $PDE$  in hypercube space with  $h = 0.2$  and determine the goodness of fit and the negative log-likelihood ratio  $\mathcal{NLLR}$ . We repeat this for an ensemble of 1000 experiments.

Figure 11(a) shows the distribution of  $s^*$  for this ensemble. The mean value of  $s^*$  over this ensemble is 49.98 gm and the RMS is 0.495 gm which is consistent with the expected  $\sigma/\sqrt{(100)}$  value of 0.5 gm. Figure 11(b) shows the distribution of  $\mathcal{NLLR}$  for the 1000 members of the ensemble. Figure 11(c) shows the likelihood ratio functions  $\mathcal{L}_R(s^*)$  for the first 10 fits in the ensemble. The

value of  $s_k^*$ , the maximum likelihood value of the  $k^{th}$  member of the ensemble fluctuates as expected, as well as the value of  $\mathcal{L}_R(s_k^*)$ , the negative logarithm of which gives the  $\mathcal{NLLR}$ . The fluctuation in  $s_k^*$  for the fits in the ensemble essentially expresses our lack of knowledge of the position of the true value  $s_T$ . The width of the likelihood distribution also contains information on the same lack of knowledge.

We now use equation 97 to obtain inverse probabilities  $P_k(s^*|\vec{c}_n)$  for each member of the ensemble. These functions are shown in Figure 11(d). The maximum likelihood value moves around with the expected spread of 0.5 gm. The average standard deviation of these curves is 0.5 gm with an rms of 0.65 E-3 gm. The average of these functions on an infinite ensemble yields the true pdf  $\mathcal{P}_n(s^*)$ .

### 7.3.8 Iterative behavior of the theory in the example

In practice, if one has a dataset with  $n = 100$  and  $N = 1000$  similar instances of them, the easiest way to analyze the data is to combine them all into a dataset with  $n' = Nn = 100,000$ . However, we are interested in studying the function  $\mathcal{P}_n(s^*)$  which is estimated by the ensemble average of the functions  $P_k(s^*|\vec{c}_n)$ . This function tells us the behavior of the distribution of the maximum likelihood values  $s^*$  over similar datasets each with  $n=100$ .

We now iterate to re-determine  $P_k(s^*|\vec{c}_n)$  and  $\mathcal{P}_n(s^*)$  as per equations 100 and 101. Figure 12(a) shows the ensemble average estimate of  $\mathcal{P}_n(s^*)$  for  $n=100$  and  $N=1000$  before and after iteration. The mean value of the uniterated and iterated functions are the same at 49.977 gm (The Gaussians were generated with a true value of 50 gm). The r.m.s values of the function

before and after iteration are 0.701 gm and 0.522 gm respectively. The iterated function thus has the correct width and mean value. Figure 12(b) shows the individual  $P_k(s^*|\vec{c}_n)$  functions for two members of the ensemble before and after iteration. The iterations pull these functions towards the true value, since we are inputting additional information on the true value. Figure 13(a) shows the values of  $s^*$  histogrammed for our illustrative example for an ensemble of  $N=1000$  and  $n=100$ . The superimposed curve is the iterated function  $\mathcal{P}_n(s^*)$  calculated for this ensemble normalized to a 1000 element ensemble. It can be seen that the function describes the distribution of  $s^*$  well. Figure 13(b) shows the iterated function  $\mathcal{P}_n(s^*)$  for  $n = 100$  and  $n = 200$  respectively. As expected, the  $n = 200$  function is narrower and its value at the maximum is larger, illustrating that  $\mathcal{P}_n(s_T)$  increases with  $n$ .

We can proceed to iteratively work out the likelihoods  $P_k(\vec{c}_n|s^*)$  and  $P(\vec{c}_n)$  as per equations 103 and 104. However, it is difficult to plot these functions since their argument is multidimensional. Instead we show how the iteration works for a special case of the above example where the dataset consists of a single measurement, i.e.  $n = 1$ . We consider an ensemble of  $N = 1000$  measurements each with a  $\sigma = 1.0$  gm. Each single measurement  $c$  is fitted to a Gaussian likelihood. The maximum likelihood point  $s^*$  is trivially equal to  $c$  and the goodness of fit likelihood ratio is always unity. The inverted probability is a Gaussian given by

$$P(s^*|c) = \frac{e^{-(s^*-c)^2/2\sigma^2}}{\sqrt{2\pi}\sigma} \quad (106)$$

We proceed to work out the function  $\mathcal{P}_n(s^*)$  by averaging the above functions over the ensemble. The resulting Gaussian will be a convolution of two Gaussians with width  $\sigma = 1.0$  and will possess a width  $\sigma = \sqrt{2}$ . Sim-

ilarly we proceed to work out  $\mathcal{P}(c)$  by averaging the theoretical likelihoods  $P_k(c|s^*)$  over the ensemble. This curve will also be too wide for similar reasons. Figure 14 shows the resulting curves for the first iteration plotted on top of the histograms for the data for  $s^*$  and  $c$  respectively. Figure 15 shows the curves after the second iteration and both the curves fit well. We now plot the resulting joint probability  $P(s^*, c)$  obtained two different ways. Figure 16 shows the joint probability worked out by the Bayes' theorem equation  $P(s^*, c) = P(c|s^*)\mathcal{P}_1(s^*)$  and Figure 17 shows the joint probability worked out by the equation  $P(s^*, c) = P(s^*|c)\mathcal{P}(c)$  after the iterations have been made. It can be seen that both these procedures give the same joint probability distribution that possesses a correlation between  $c$  and  $s^*$  that is less extreme than the initial correlation of  $c = s^*$ . The projections of the joint probability on the  $c$  and the  $s^*$  axes fit the data well. We have iteratively solved Bayes' theorem on the ensemble and inverted the probability correctly without the use of a Bayesian prior.

#### 7.4 *The two different methods to obtain $\mathcal{P}_n(s^*)$*

In our theory,  $\mathcal{P}_n(s^*)$  is the function obtained by histogramming the maximum likelihood values  $s_k^*$  for an infinite ensemble of datasets  $\vec{c}_n$  and normalizing the resulting histogram to unity. i.e. it is the probability density function of the maximum likelihood values on the ensemble, for datasets each containing  $n$  elements. However, equation 99 shows another way of obtaining the same function. What is the connection between the two methods?

Without loss of generality, we can express the inverse probability function as

a function of  $s^* - s_k^*$  such that

$$P_k(s^*|\vec{c}_n) \equiv \mathcal{G}_k(s^* - s_k^*) \quad (107)$$

Then equation 99 can be re-expressed

$$\mathcal{P}_n(s^*) = \lim_{N \rightarrow \infty} \frac{1}{N} \sum_{k=1}^{k=N} \mathcal{G}_k(s^* - s_k^*) \quad (108)$$

But this is just the probability density estimator (*PDE*) for the distribution of  $s^*$ , with the functions  $\mathcal{G}_k$  serving as the kernels!. They satisfy the normalization condition  $\int \mathcal{G}_k(t)dt = 1$  as required. This should be compared with equation 51 for the definition of *PDE's*. Thus  $\mathcal{P}_n(s^*)$  represents a *PDE* of the distribution of  $s^*$  and will yield the same distribution as  $s^*$ .

In the limit  $N \rightarrow \infty$ , we can represent the distribution of the maximum likelihood values  $s^*$  on the ensemble as the continuous *pdf*  $\mathcal{P}_n(s^*)$ . In this limit, one can write

$$\mathcal{P}_n(s^*) = \int \mathcal{P}_n(s^{*'}) \mathcal{G}(s^{*'}, s^* - s^{*'}) ds^{*'} \quad (109)$$

where we have used the notation  $\mathcal{G}(s^{*'}, s^* - s^{*'})$  to emphasize the variation of the kernel as a function of  $s^{*'}$  (i.e. ensemble element). The latter half of the above equation is an integral equation with kernel  $\mathcal{G}(s^{*'}, s^* - s^{*'})$  whose eigenfunction is  $\mathcal{P}_n(s^*)$ .

Let us also note that the iterative method used to solve Bayes' theorem in the example given above where  $c = s^*$ , can be used as a *PDE* method to adjust the kernels by changing their shape iteratively without resort to an adjustable parameter  $h$ . We could have fed in data generated as an exponential(for example) with the assumption that each measurement has a Gaussian error.

Then each of the Gaussian kernels would have been altered by the resulting exponential function  $\mathcal{P}_n(s^*)$  iteratively yielding a PDE for the exponential.

### 7.5 Co-ordinate transformations $s^{*'} = s^*(s^*)$

The inverse probability density functions  $P(s^*|\vec{c}_n)$  are invariant under the co-ordinate transformations  $c' = c'(c)$ . How do they behave under transformations  $s^{*'} = s^*(s^*)$ ? The function  $P_k(s^*|\vec{c}_n)$  represents our estimate using one member of the ensemble of the *pdf* of  $s^*$ . So if  $P_k(s^*|\vec{c}_n)$  represents a *pdf*, we would expect it to behave like a *pdf*, namely

$$P_k(s^{*'}|\vec{c}_n) = P(s^*|\vec{c}_n) \left| \frac{\partial s^*}{\partial s^{*'}} \right| \quad (110)$$

This is how *pdf's* transform (via the Jacobian). This can be shown patently not to be so, since  $P_k(\vec{c}_n|s^{*'}) = P_k(\vec{c}_n|s^*)$  and

$$P_k(s^{*'}|\vec{c}_n) = \frac{P_k(\vec{c}_n|s^{*'})}{\int P_k(\vec{c}_n|s^{*'}) ds^{*'}} = \lambda_k(\vec{c}_n) P_k(s^*|\vec{c}_n) \quad (111)$$

where the  $s^*$  independent constant  $\lambda_k(\vec{c}_n)$  is given by

$$\lambda_k(\vec{c}_n) = \frac{\int P_k(\vec{c}_n|s^*) ds^*}{\int P_k(\vec{c}_n|s^{*'}) ds^{*'}} \quad (112)$$

i.e. the inverse probability densities do not transform in a way that is expected of *pdf's*. This was perhaps a naive expectation. As we have just demonstrated, the inverse probability densities serve the purpose of kernels on the ensemble, the ensemble average of which gives the *pdf*  $\mathcal{P}_n(s^*)$ . There is no need for the kernel from a member of the ensemble to transform to the kernel from the same member under these transformations. The properties of the ensemble

average deduced from the individual kernels will fluctuate from kernel to kernel. Similarly, when one analyzes in transformed variables, the same kernel will give different results which may be thought of as being part of the fluctuation.

The distributions of the maximum likelihoods  $\mathcal{P}_n(s^*)$  however will transform as *pdf's*, since  $\mathcal{P}_n(s^*)$  represents the probability density of the maximum likelihood value and  $s'^* = s'(s^*)$ . i.e.

$$\mathcal{P}'_n(s'^*) = \left| \frac{\partial s^*}{\partial s'^*} \right| \mathcal{P}_n(s^*) \quad (113)$$

The transformed kernels *after iteration* will yield the transformed  $\mathcal{P}'_n(s'^*)$ .

### 7.5.1 Comparison with the Bayesian approach

Table 2 outlines the major differences between the Bayesian approach and the new paradigm.

## 8 Conclusions

To conclude, we have proposed a general theory for obtaining the goodness of fit in likelihood fits for both binned and unbinned likelihood fits. In order to obtain a goodness of fit measure, one needs two likelihoods:- one derived from theory and the other derived from the data alone. In order to compute the errors on fitted quantities, inverse probability densities need to be worked out and Bayes' theorem needs to be employed. Using insights gained in solving the goodness of fit problem, we demonstrate that it is possible to estimate the inverse probability densities without the use of Bayesian prior. This results in a new paradigm in statistics.

Table 2

The key points of difference between the Bayesian method and the new method.

Item	Bayesian Method	New Method
Goodness of fit	Absent	Now available  in both binned  and unbinned fits
Data	Used in evaluating  theory <i>pdf</i>  at data points	Used in evaluating  theory <i>pdf</i>  at data points  as well as evaluating  data <i>pdf</i> at data points
Prior	Is a distribution  that is guessed based  on “degrees of belief”  Independent of data,  monolithic	No prior needed.  One calculates a  constant from data  $\mathcal{P}_n(s_T) = \frac{P^{data}(\vec{c}_n)}{\int P(\vec{c}_n s^*) ds^*}$  $\rightarrow \infty$ as $n \rightarrow \infty$
Inverse probability density	Depends on Prior.  $P(s \vec{c}_n) = \frac{P(\vec{c}_n s)P(s)}{\int P(\vec{c}_n s')P(s') ds'}$	Independent of prior.  same as frequentists use  $P(s^* \vec{c}_n) = \frac{P(\vec{c}_n s^*)}{\int P(\vec{c}_n s') ds'}$



## 9 Acknowledgments

This work is supported by Department of Energy.

## 10 Appendix

In order to demonstrate the capabilities of the unbinned goodness of fit method, we illustrate its power with the following example.

### 10.1 *An extreme problem*

We now attempt to solve a problem with three observed data points, made extreme due to the sparsity of data. The problem is stated as follows.

“Three data points are observed [15] in three dimensional co-ordinate space  $x, y, z$  with  $(x, y, z) = (0.1, 0.2, 0.3)$ ,  $(0.2, 0.4, 0.1)$ , and  $(0.05, 0.6, 0.21)$ . What is the goodness of fit to the hypothesis that the observed number of events is distributed according to  $p(x, y, z) = e^{-(x+y+z)}$  ?”

### 10.2 *Goodness of fit for the above problem*

We note that the likelihood function for the problem is

$$\mathcal{L} = \prod_{i=1}^{i=3} \frac{1}{s} \exp - ((x_i + y_i + z_i)/s) \quad (114)$$

where we assume a maximum likelihood fit has been done and the lifetime parameter  $s$  has been determined to be  $s^* = 1$  at the maximum. Since the

three co-ordinates x,y, and z are uncorrelated (as per the above likelihood function), we can reformulate the problem as a single dimensional problem as follows.

$$\mathcal{L} = \prod_{i=1}^{i=9} \frac{1}{s} \exp(-c_i/s) \quad (115)$$

where the n=9 vector  $\vec{c}_n = 0.1 \ 0.2 \ 0.3 \ 0.2 \ 0.4 \ 0.1 \ 0.05 \ 0.6 \ 0.21$

We transform the co-ordinates to the hypercube space ( $s^* = 1$ ), with the limits of  $c$  assumed to be 0.0 and 10.0<sup>1</sup>.

Figure 18 shows the transformed co-ordinates in hypercube space. We then proceed to work out the negative log-likelihood ratio  $\mathcal{NLLR}$  for this configuration with the “smoothing parameter  $h$ ” set to three different values  $h = 0.2, 0.3$  and  $0.4$ . We study the behavior of the  $\mathcal{NLLR}$  for the null hypothesis (i.e. n=9 events distributed uniformly in hypercube space) for a 1000 such experiments. We repeat this for a dataset of  $n = 100$  as well to study the effect of the small data sample on our goodness of fit measure. Figure 19 shows the distribution of the  $\mathcal{NLLR}$  for the three different values of  $h$  for a data set size  $n = 9$ . Figure 20 shows the distribution of the  $\mathcal{NLLR}$  for the three different values of  $h$  for a data set size  $n = 100$ . Table 3 summarizes the observed  $\mathcal{NLLR}$  for our dataset as a function of  $h$ . The mean and sigma of the null hypothesis histograms are also shown as well as the probability that the observed  $\mathcal{NLLR}$  is exceeded for both the  $n = 9$  null hypothesis and an  $n = 100$  null hypothesis. The latter is run to test the sensitivity of the results to the small data sample.

---

<sup>1</sup> Since the program expects a finite upper limit, the high value of  $c=10$  is deemed to be sufficiently large to be infinite for this problem.

Table 3

Summary of results

Smoothing parameter $h$	Dataset $\mathcal{NLLR}$	n=9 $\mu$	n=9 $\sigma$	n=9 Prob. to exceed	n=100 $\mu$	n=100 $\sigma$	n=100 Prob. to exceed
0.2	5.36	0.82	1.26	0.5%	0.77	1.255	0.3%
0.3	5.84	0.34	0.96	< 0.1%	0.30	0.91	< 0.1%
0.4	1.77	0.12	0.67	1.0%	0.083	0.697	1.1%

### 10.3 Comments

The observed data is a bad fit to the model. We have managed not only obtain a goodness of fit for the problem (made extreme by the sparsity of data), but also to show that the method gives reliable results for a variety of smoothing parameters. The method is also robust with respect to the data size  $n$ . We see that as we increase the smoothing parameter to 0.4, we begin to increase the chance of fitting. When  $h = 1.0$ , everything will fit. A smoothing parameter of  $h = 0.2$  or  $0.3$  gives reliable results. The probability to exceed the observed  $\mathcal{NLLR}$  is estimated from the histograms with 1000 experiments. We can improve the accuracy of this by running more Monte Carlo statistics.

## References

- [1] R. A. Fisher, “On the mathematical foundations of theoretical statistics”, *Philos. Trans. R. Soc. London Ser. A* **222**, 309-368(1922);  
R. A. Fisher, “Theory of statistical estimation”, *Proc. Cambridge Philos. Soc.* **22**, 700-725 (1925).

- [2] E. Parzen, “On estimation of a probability density function and mode”  
*Ann.Math.Statis.* **32**, 1065-1072 (1962).
- [3] J. Neyman and E. S. Pearson, *Biometrika* 20A (1928) 263. See also S. Brandt,  
“Statistical and Computational Methods in Data Analysis”, Springer, New York,  
(1997) for a proof.
- [4] S. Baker, R. D. Cousins, *Nucl. Instrum. Meth.* A221 (1984).
- [5] See P. G. Hoel, “Introduction to Mathematical Statistics”, 4<sup>th</sup> ed., Wiley, New  
York 1971, p211 for a derivation of the likelihood ratio theorem.
- [6] D. Scott. *Multivariate Density Estimation*. John Wiley & Sons, 1992.  
M. Wand and M. Jones, *Kernel Smoothing*. Chapman & Hall, 1995.
- [7] “An essay towards solving a problem in the doctrine of chances”,  
Rev. Thomas Bayes, *Biometrika*, **45** 293-315 (Reprint of 1763) (1958).
- [8] Empirically we found that a power of the order of -0.6 is needed to provide  
sufficiently large smoothing factors for large values of time. We can in principle  
optimize this smoothing function further, but have not done so.
- [9] Objective Bayesianism may first have been proposed by Pierre-Simon, Marquis  
de Laplace, “Theorie Analytique des Probabilite” (1812).  
See also E. T. Jaynes, “Probability Theory: The Logic of Science”, for a more  
modern treatment of objective Bayesianism.
- [10] Bruno De Finetti, “Theory of Probability, A Critical Introductory treatment”,  
John Wiley & Sons, (1974)
- [11] For a description of hierarchical Bayesian formalism, see Bradley P. Carlin and  
Thomas A. Louis, “Bayes and Empirical Bayes Methods for Data Analysis”,  
Chapman & Hall/CRC, Page 19.

- [12] C. N. Morris, “Parametric empirical Bayes inference: Theory and applications”,  
J.Amer.Statist.Assoc.,**78**,47-65.
- [13] All Bayesians make this substitution. See for example De Finetti [10] P. 142.
- [14] R. A. Fisher, “The Fiducial Argument in Statistical Inference”, Annals of  
Eugenics, 6:391-398(1935).
- [15] The author is grateful to Bruce Knuteson for posing this problem.

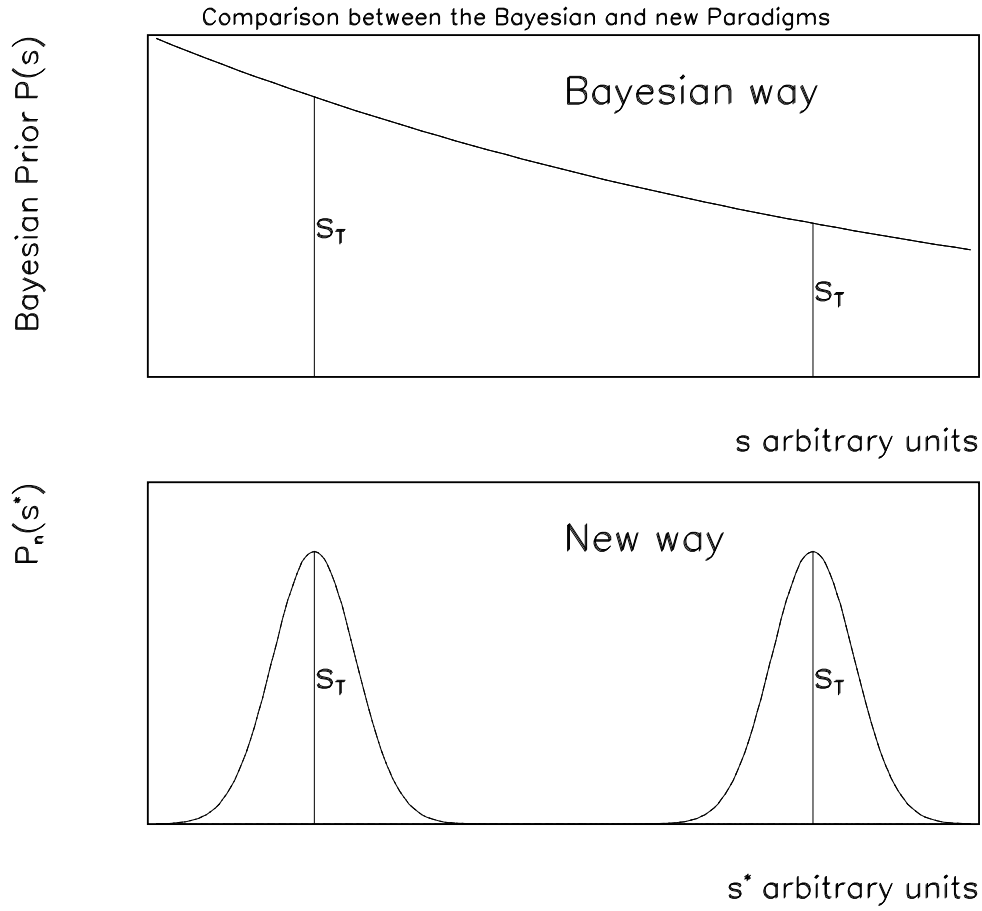


Fig. 10. Comparison of the usage of Bayesian priors with the new method. In the upper figure, illustrating the Bayesian method, an unknown distribution is guessed at by the user based on “degrees of belief” and the value of the Bayesian prior changes as the variable  $s$  changes. In the lower figure, an “unknown concomitant” distribution  $\mathcal{P}_n(s^*)$  is used whose shape depends on the statistics of the dataset  $\vec{c}_n$ . In the case of no bias, this distribution peaks at the true value  $s_T$ . As we change  $s^*$ , we change our hypothesis as to where the true value of  $s$  lies, and the distribution shifts with  $s^*$  as explained in the text. The value of the distribution at the true value is thus independent of  $s^*$ .

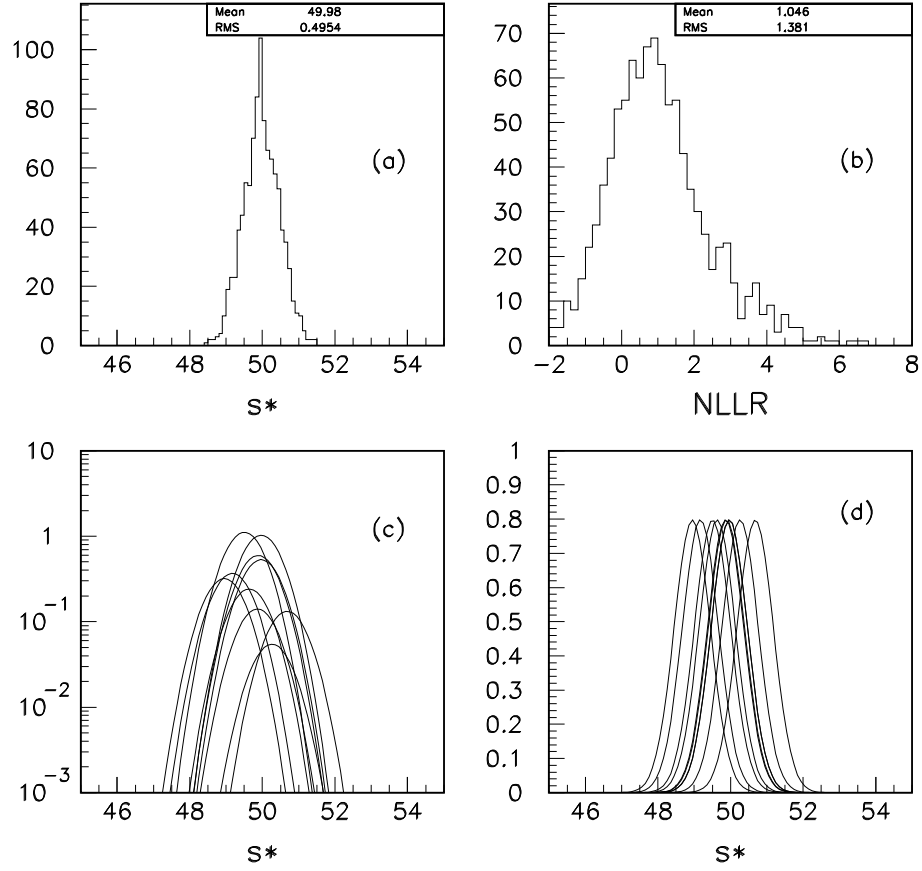


Fig. 11. (a) The distribution of  $s^*$ , the maximum likelihood value of  $s$  for a 1000 member ensemble of datasets of  $n = 100$ . (b) The goodness of fit variable  $\mathcal{NLLR}$  for the fits (c) The likelihood ratio  $\mathcal{L}_R(s^*)$  as a function of  $s^*$  for the first 10 members of the ensemble (d) The function  $P(s^*|\vec{c}_n)$  for the first 10 members of the ensemble.

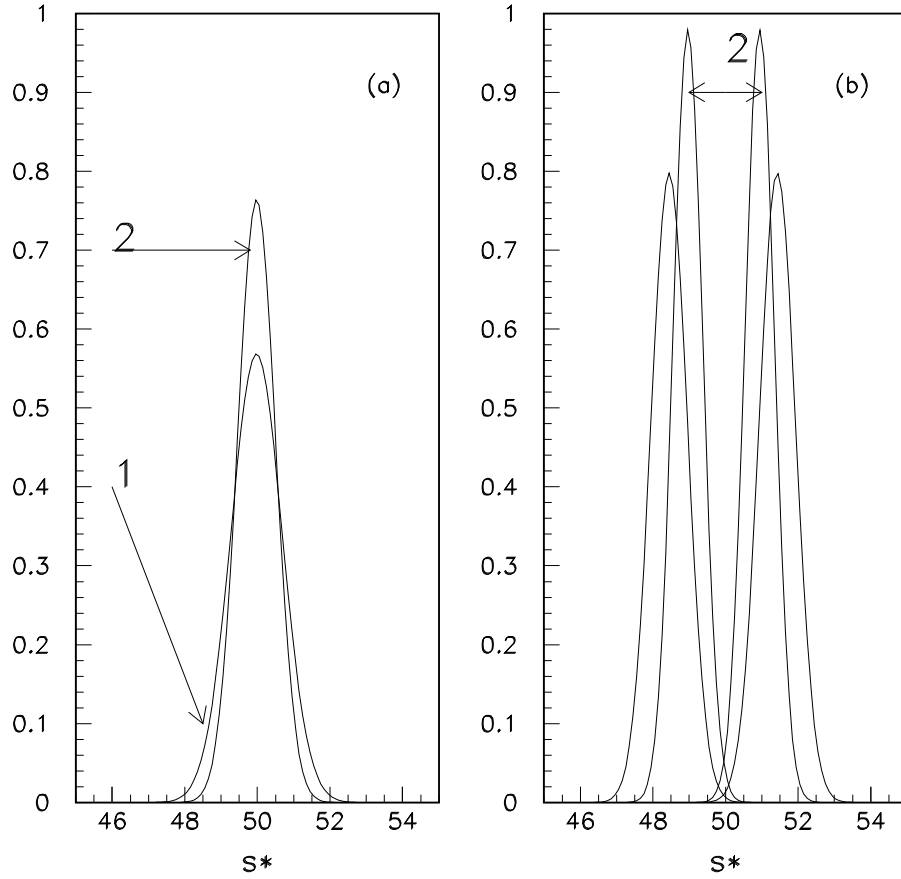


Fig. 12. (a) The function  $\mathcal{P}_n(s^*)$  computed on the ensemble for  $n=100$  and  $N=1000$ . The two iterations are shown, with the numbers (1,2) indicating the iteration number. (b) The function  $P(s^*|\vec{c}_n)$  for two elements on the ensemble for the two iterations.



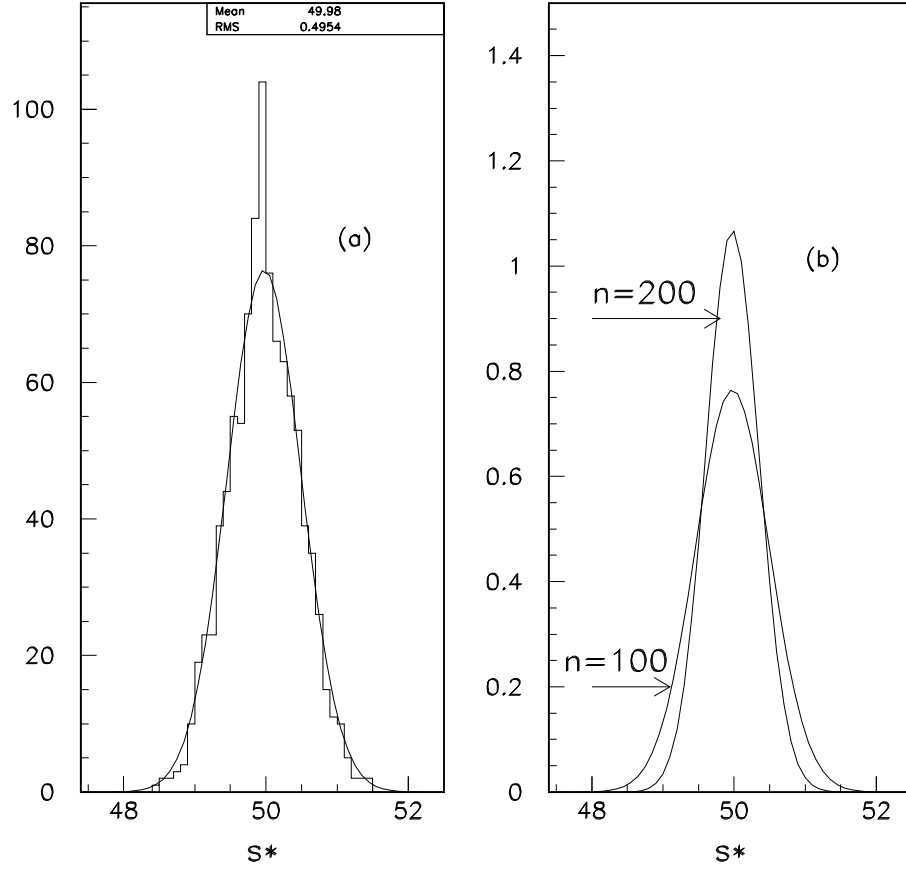


Fig. 13. (a) The distribution of  $s^*$  (solid histogram) for an ensemble with  $N=1000$  elements each consisting of a dataset  $n=100$ . The curve is the estimate for the iterated function  $\mathcal{P}_n(s^*)$  for this ensemble normalized to the 1000 observations. (b)  $\mathcal{P}_n(s^*)$  on the ensemble for  $n=100$  and  $n=200$ . This illustrates that the ensemble averaged function, depends on  $n$ , the size of the dataset. As  $n$  increases, the function narrows and the value of the function at its maximum increases.

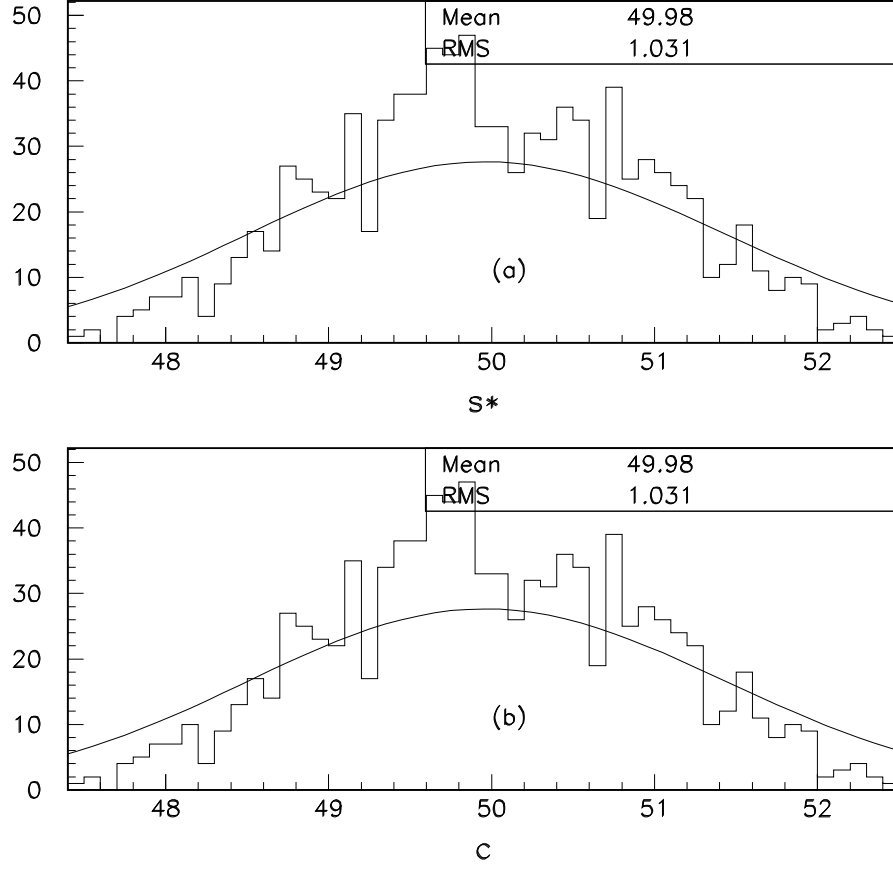


Fig. 14. (a) Histogram of  $s^*$  values over an ensemble of  $N=1000$ . Superimposed is our first iteration of the function  $\mathcal{P}_n(s^*)$ . (b) Histogram of  $c$  values over an ensemble of  $N=1000$ . Superimposed is our first iteration for the function  $P(c)$ . The RMS values refer to the width of the histogram. The first iteration curves are too wide as explained in the text.

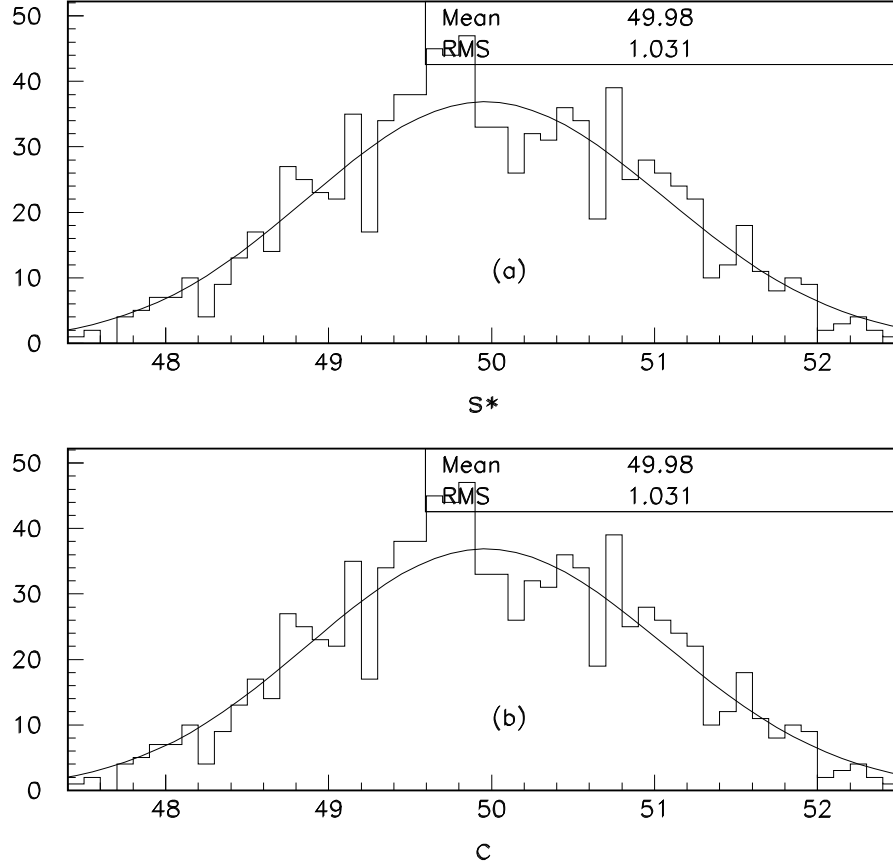


Fig. 15. (a) Histogram of  $s^*$  values over an ensemble of  $N=1000$ . Superimposed is our second iteration of the function  $\mathcal{P}_n(s^*)$ . (b) Histogram of  $c$  values over an ensemble of  $N=1000$ . Superimposed is our second iteration for the function  $P(c)$ .

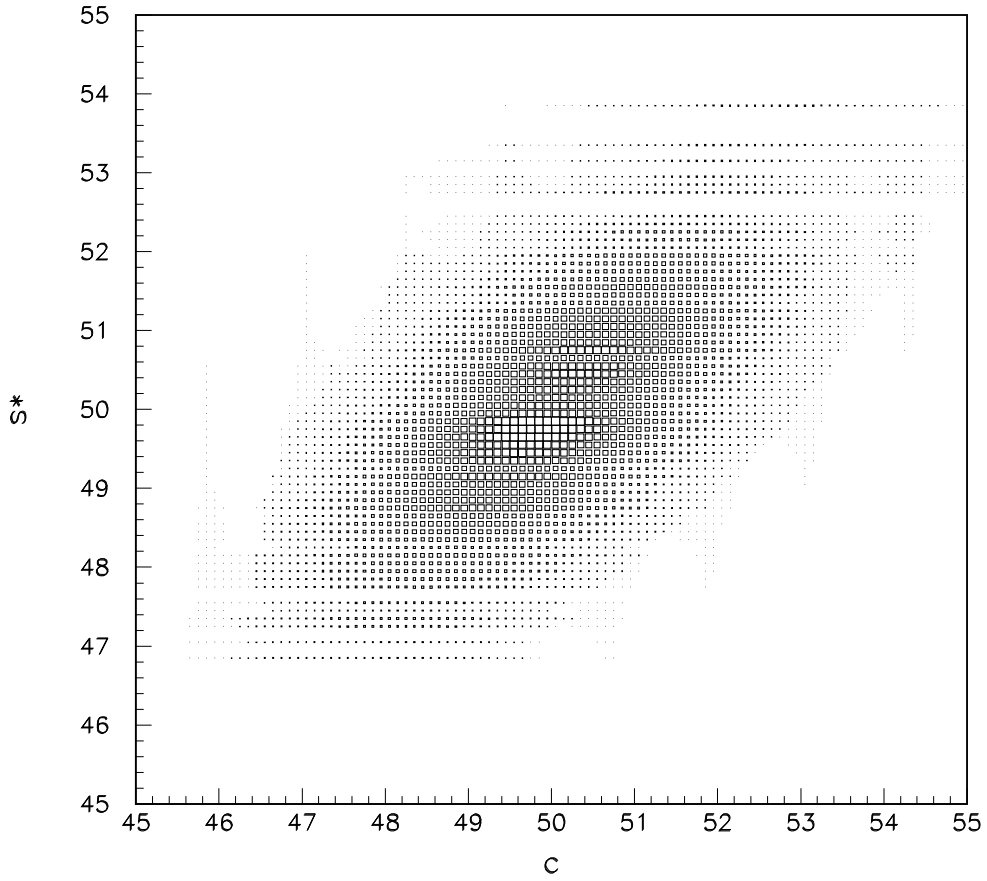


Fig. 16. Joint probability  $P(c, s^*)$  computed from  $P(c|s^*)P(s^*)$  at the end of two iterations

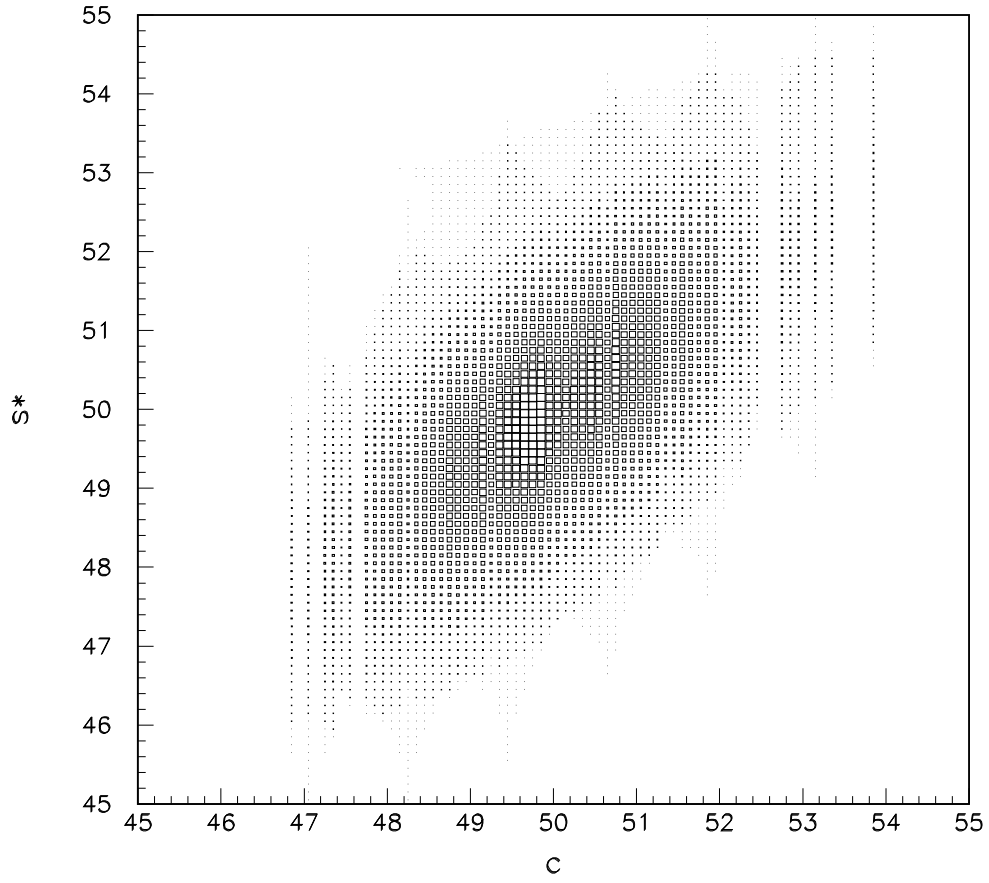


Fig. 17. Joint probability  $P(c, s^*)$  computed from  $P(s^*|c)P(c)$  at the end of two iterations

2005/06/24 15.24

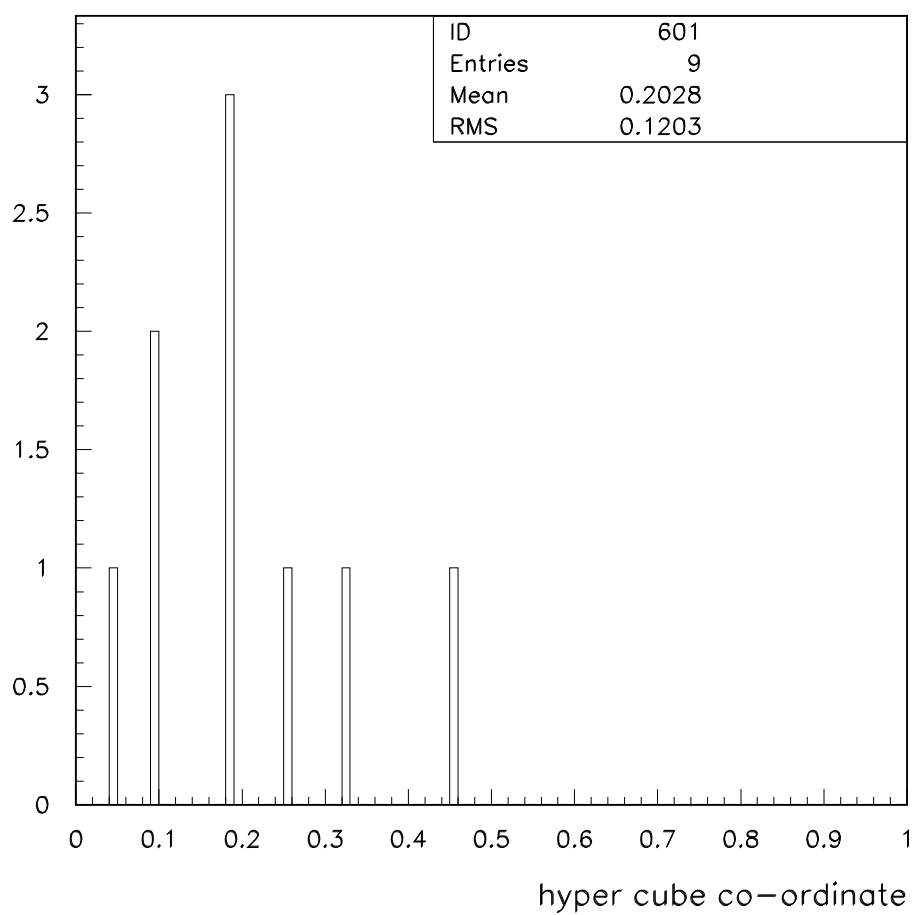


Fig. 18. Transformed co-ordinates in hypercube space.

2005/06/24 15.24

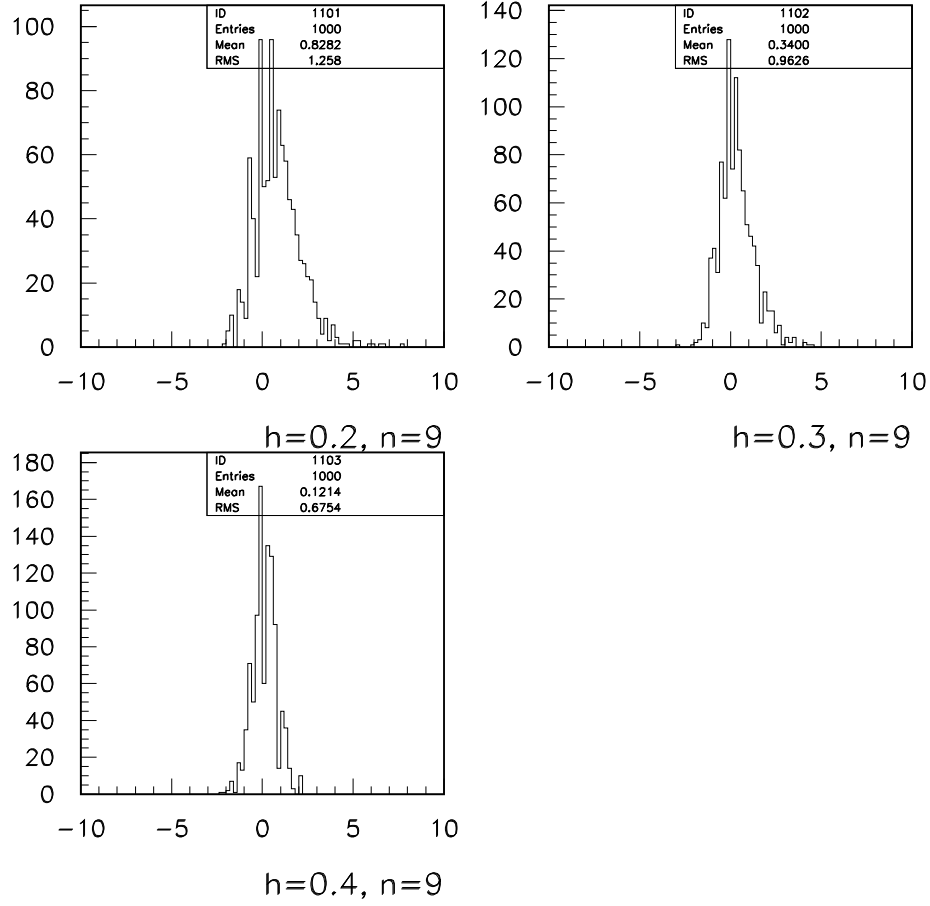


Fig. 19. The distribution of  $\mathcal{NLLR}$  as a function of the smoothing parameter  $h = 0.2, 0.3, 0.4$  for a dataset  $n = 9$  generated to be uniform in the hypercube.

2005/06/24 15.24

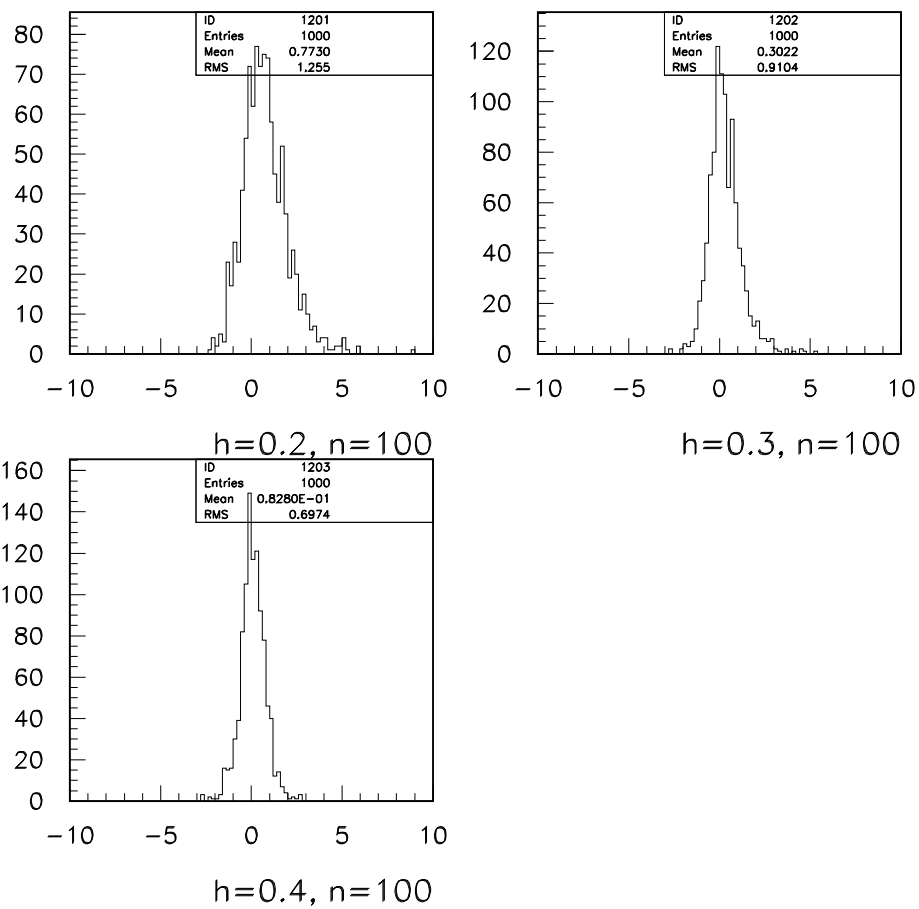


Fig. 20. The distribution of  $\mathcal{NLLR}$  as a function of the smoothing parameter  $h = 0.2, 0.3, 0.4$  for a dataset  $n = 100$  generated to be uniform in the hypercube.